

1 *Review*

2 Environmental Remediation Applications of Carbon 3 Nanotube and Graphene Oxide: Adsorption and 4 Catalysis

5 Yanqing Wang ^{1,2,3,*}, Can Pan ⁴, Adavan Kiliyankil Vipin ², Ling Sun ^{5,*} and Wei Chu ⁴6 ¹ Nihon Trim Co., Ltd., 2-2-22 Umeda, Kita-ku, Osaka 530-0001, Japan; y.wang@ipr-ctr.t.u-tokyo.ac.jp
7 (Y.Q.W.)8 ² School of Engineering, The University of Tokyo, Bunkyo-ku, Tokyo, 113-0032, Japan; vipin@ipr-ctr.t.u-
9 tokyo.ac.jp (A.K.V.)10 ³ College of Polymer Science and Engineering, State Key Laboratory of Polymer Material and Engineering,
11 Sichuan University, Chengdu 610065, China12 ⁴ School of Chemical Engineering, Sichuan University, Chengdu 610065, China; 15053108110@163.com
13 (C.P.); chuwei1965@foxmail.com (W.C.)14 ⁵ Beijing Guyue New Materials Research Institute, Beijing University of Technology, 100 Pingleyuan,
15 Chaoyang District, Beijing 100124, China; sunling@bjut.edu.cn

16 * Correspondence: y.wang@ipr-ctr.t.u-tokyo.ac.jp; sunling@bjut.edu.cn; Tel.: +81-3-5841-7461

17 Received: date; Accepted: date; Published: date

18 **Abstract:** Environmental issues such as the wastewater have influenced each aspect of our lives.
19 Coupling the existing remediation solutions with exploring new functional carbon nanomaterials
20 (e.g. carbon nanotube, graphene oxide, graphene) by various perspectives shall open up a new
21 venue to understand the environmental issues, phenomenon and find out the ways to get along
22 with the nature. This review makes an attempt to provide an overview of potential environmental
23 remediation solutions to the diverse challenges happening by using low-dimensional carbon
24 nanomaterials and their composites as adsorbents, catalysts or catalysts support towards for the
25 social sustainability.

26 **Keywords:** carbon nanomaterials; graphene oxide; graphene; carbon nanotube; environmental
27 remediation; adsorption; catalysis

29 1. Introduction

30 Along with the growing population, industrialization and urbanization, the lack of fresh and
31 clean water is becoming a ubiquitous problem around the world [1-4]. Meanwhile, the shortage of
32 water resources calls for efficient technologies for decontamination of wastewater, as well as the
33 technologies for the seawater desalination. Hydrogen-dissolved water (electrochemically reduced
34 water) studies performing high functionality are recently in hot topic [5,6]. Not to mention, over one
35 half of the world population, mainly in Asia has to face a severe scarcity of safe water[7].
36 Environmental preservation has become a matter of major social concern. Although a lot of
37 legislations have been imposed on effluent discharges, effective remediation processes are still highly
38 desired to deal with non-readily biodegradable and toxic pollutants. It's well known dyes are usually
39 used in textile manufacture, printing industry, and biochemical project, etc. Besides, that color
40 removal with respect to organic effluents in discharged wastewater has been a compulsory measure
41 and otherwise pertains to an illegal behavior[8]. The search for safe, effective and economic materials
42 that can eliminate the current and future environmental contaminations from water is a scientific and
43 technological issue of primary importance to the whole scientific community. Scientists around the

44 world are devoting to find out effective materials either from natural or synthetic all for one purpose
45 of environmental remediation.

46 Low-dimensional **novel** carbon nanomaterials e.g. carbon nanotubes (CNTs) and graphene
47 oxide (GO) have been stimulating enormous interest in various scientific communities ever since their
48 discovery. CNTs are a potential material used for a variety of applications because of its exceptional
49 physical and chemical properties. The applications of CNTs are not limed to electrical, electronics,
50 sensors, and thermal devices; moreover, they are emerging **materials** for environmental remediation
51 [9-12]. CNTs are indeed a new class of material useful for environmental applications because of their
52 cylindrical hollow structure, large surface area, high **length to radius ratio**, and hydrophobic wall and
53 surface **that can be easily modified** [13]. GO is one **oxidized analog** of graphene, recognized as the
54 promising intermediate for obtaining the latter in large scale[14], since Brodie **centuries ago** first
55 reported about the oxidation of graphite [15]. Three decades **earlier**, one atom-thin single layer of
56 graphite was officially defined with the term graphene [16], structurally comprising sp^2 hybridized
57 carbon atoms arranged in a honeycomb lattice, **characterized by** promising properties in terms of
58 mechanical, electrical, and **other**[17-19]. Despite well-known properties, GO remains limited success
59 in practical applications, mainly due to the difficulties in large-scale production of desired highly-
60 organized structure[20]. While as one promising precursor, GO was much **emphasized by**
61 **academicians** and **by industry** in **the last** decades [21,22], because it is readily exfoliated from bulk
62 graphite oxide [23]. Such bottom-down strategy features **of utmost** flexibility and effectiveness **arouse**
63 **great** interest in its practical applications.

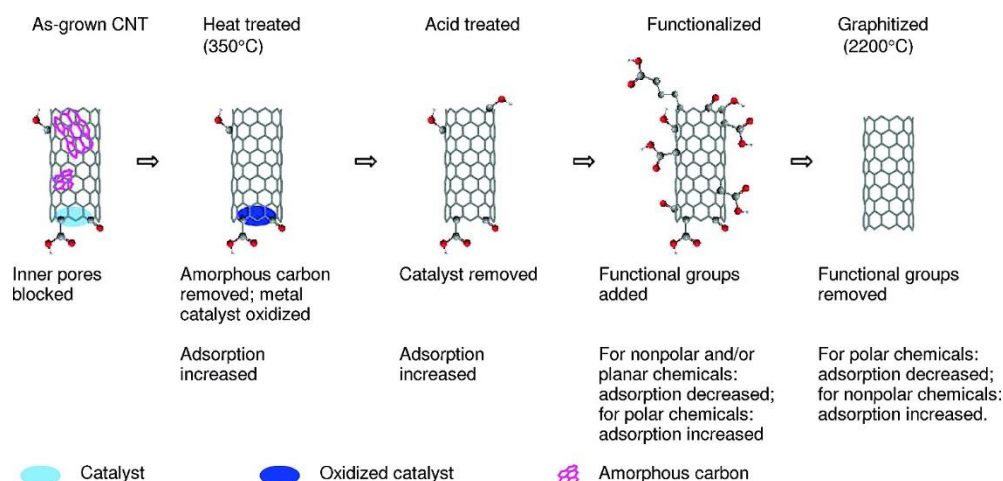
64 Up to now, there are some reviews discussing about the recent advances in low-dimensional
65 carbon nanomaterials such as carbon nanotubes, graphene oxide, and graphene derivatives in terms
66 of wastewater treatment[4,11,12,24-33]. However, the effective design of multifunctional carbon
67 nanomaterials **via structural engineering, morphological control and component manipulation** and
68 get the utmost of them **in the matrix** during the application **need** to be paid more attention. **Therefore**,
69 this review **is intended** to highlight the **effect of functionalization and / or** encapsulation of CNTs and
70 GO in **individual** or **complex** states, facilitating **the effectiveness of** various environmental
71 remediation **techniques**.

72 2. Carbon nanotubes (CNTs) based composite materials for water remediation

73 2.1 CNTs / functionalized CNTs as **sorbents**

74 CNTs were considered as a superior material for the remediation of a wide range of organic and
75 inorganic contaminants comparing with conventional sorbents such as clay, zeolite, and activated
76 carbon, because of their stronger chemical **and physical** interactions, rapid equilibrium, high sorbent
77 capacity, and tailored surface chemistry[34,35]. Here we summarize the research achievements of
78 CNTs in environmental remediation. We mainly addressed this section in two parts, **concerning**
79 remediation of organic and inorganic pollutants.

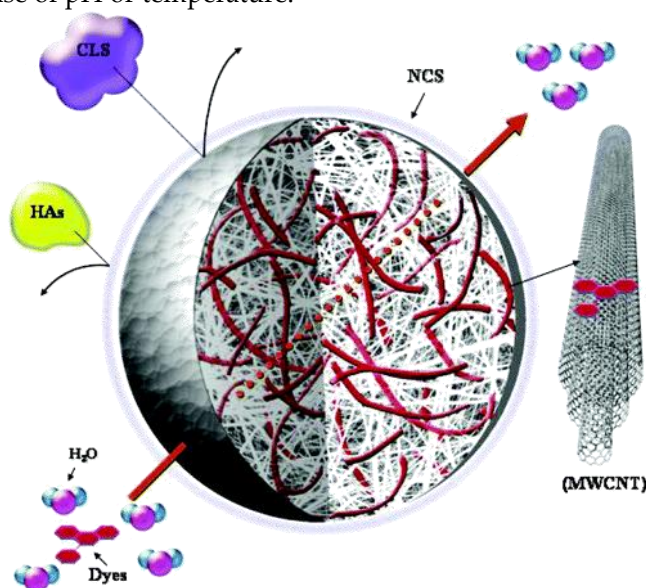
80 **Adsorption mechanisms of organic molecules on CNTs have been extensively studied. Multiple**
81 **mechanisms are acting simultaneously such as hydrophobic interactions on the surface of CNTs, π -**
82 **π interactions, hydrogen bonds, and electrostatic interactions[36]. The adsorption of organic**
83 **molecules on CNTs is mainly affected by the morphology and functional groups of CNTs and organic**
84 **molecules. The adsorption also depends on the defects and active sites of CNTs[37]. Other**
85 **environmental parameters that affected the adsorption are pH, ionic strength and dispersion state of**
86 **CNTs[13]. The surfaces of raw CNTs are hydrophobic and show strong preference for adsorption of**
87 **hydrocarbons (e.g., hexane, benzene, and cyclohexane), over alcohols (e.g., ethanol, 2-propanol).**
88 **Surface functionalization reduces (usually) hydrophobicity, increases oxygen content, decreases**
89 **specific surface area and, as a result, reduces adsorption of nonpolar hydrocarbons. Similarly**
90 **adsorption of planar chemicals also decreases due to insufficient contact between CNTs and the**
91 **chemicals. Adsorption properties as affected by CNT functional groups are shown in Figure 1.**



92
93 **Figure 1. The general trend for the changes of CNT adsorption properties after different treatments.**
94 **Reprinted with permission from [36]. Copyright (2008) American Chemical Society.**

95 **Organic Dyes**

96 The first use of mono-dispersed CNTs as the active elements for the elimination of dyes was
97 reported by Fugetsu et al.[38]. They developed a Ba²⁺-alginate matrix **constituting** a cage, which holds
98 the physically trapped multi-wall carbon nanotubes (MWCNTs) (Figure 2). The beads carry negative
99 charges on **their** surface so that they were capable for the elimination of cationic dyes such as acridine
100 orange (AO), ethidium bromide (EB), eosin bluish (EOB), and orange G (OG). The adsorption
101 efficiency of MWCNTs encapsulated by barium alginate beads for **AO, EB, EOB and OG** were 0.44,
102 0.43, 0.33 and 0.31 μmol/mg, respectively. Chung-Hsin Wu examined the adsorption efficiency of
103 MWCNTs for **procion red MX-5B** at various pH and temperatures. The **saturation** adsorption
104 capacity was 44.64 mg/g without any modification of MWCNTs[39]. The adsorption of dye on CNTs
105 decreased with an increase of pH or temperature.



106
107 **Figure 2. Schematic representation of the advantageous performances of the caged MWCNTs on**
108 **dye adsorption. Reprinted with permission from [38]. Copyright (2008) American Chemical Society.**

109 Ghaedi et al. did a comparative study of activated carbon and MWCNTs for efficient removal of
110 Eriochrome Cyanine R (ECR). They **studied the kinetics in detail, isotherms, and thermodynamics**
111 and observed that pH is important **factor** controlling adsorption. MWCNT in comparison with
112 **activated carbon (AC)** has a higher adsorption capacity, and it reaches equilibrium in a shorter time.
113 Physical forces, as well as ionic interaction, are responsible for the binding of ECR material[40]. Azo
114 dyes are the most common synthetic dyes used in **dye-works in the textile industry** and the efficiency
115 of MWCNTs as an adsorbent for removal of **acid red 18 (AR18)** from aqueous solution was
116 determined. The research found that the Langmuir was the best fitted for experimental data with

117 maximum adsorption capacity of 166.67 mg/g and the rate of adsorption was observed close to
118 pseudo-second-order compared to other kinetic models[41].

119 Decontamination of cationic methylene blue from aqueous solution using carbon nanotubes was
120 extensively investigated[42]. The adsorption capacity increased with temperature due to the
121 endothermic nature of adsorption for CNTs and increasing mobility of dye molecules. They got a
122 fantastic adsorption capacity of 132.6 mg g⁻¹ at 310 K[43]. The integration of MWCNTs with
123 Fe₂O₃ nanoparticles has great potential application to remove neutral red (NR) along with methylene
124 blue (MB). The adsorption capacities for MB and NR are 42.3 mg/g and 77.5 mg/g, respectively[44].
125 Iiguez et al. researched the removal of MB together with Orange II (OII) anionic dye, from an aqueous
126 solution by using MWCNTs. From the overall results, they concluded that MWCNTs could
127 effectively remove both cationic and anionic dyes from aqueous solutions[45]. Gong et al. developed
128 a magnetic multi-wall carbon nanotube nanocomposite for the removal of cationic dyes such as MB,
129 NR, and brilliant cresyl blue (BCB) from aqueous solution [46]. Similarly, a magnetic polymer multi-
130 wall carbon nanotube nanocomposite was developed by Gao et al. for anionic azo dyes removal[47].
131 Those composites were relatively easy to separate from the solution after adsorption using a magnet.
132 CNTs based composites for adsorption of dyes were also reported, it is CNT–chitosan, CNT–
133 activated carbon fiber (ACF), CNTs–Fe₃O₄, CNTs–dolomite, CNTs–cellulose, and CNTs–graphene
134 [13,48,49].

135 *Other organic pollutants*

136 Chen et al. conducted systematic study on the adsorption of polar and nonpolar organic
137 chemicals on CNTs. The adsorption increased in the order of nonpolar aliphatic < nonpolar aromatics
138 < nitroaromatics; whereas, the adsorption affinity increased with the number of nitro functional
139 groups[50]. The first systematic study on the adsorption of polycyclic aromatic hydrocarbons such as
140 naphthalene, phenanthrene, and pyrene onto six carbon nanomaterials, including single-wall carbon
141 nanotubes (SWCNTs) and MWCNTs, was investigated by Kun Yang group[51]. A linear relationship
142 between adsorbed capacities and surface areas or micropore volumes of these carbon nanomaterials
143 is obtained. Agnihotri et al. studied the adsorption of organic vapors on SWCNTs such as toluene,
144 methyl ethyl ketone (MEK), hexane and cyclohexane. The relative adsorption capacities was in the
145 order of toluene (maximum) > MEK > hexane > cyclohexane[52]. Similarly, SWCNT interactions with
146 aromatic (benzene), aromatic and heterocyclic (thiophene), and nonaromatic (cyclohexane) molecules
147 were investigated by Dennis Crespo and Ralph T. Yang. The strongest adsorption was observed for
148 smaller SWCNTs, and the adsorption followed the order thiophene > benzene > cyclohexane[53].

149 Hazardous and carcinogenic trihalomethanes (THMs), the important (organic) contaminants has
150 to be of primary interest.. However, CNTs were purified by acid solution and effectively used for the
151 adsorption of THMs from the water[54]. The polyaniline (PANI) grafted onto MWCNTs by plasma-
152 induced grafting technique were successfully developed by Shao et al. PANI/MWCNTs have very
153 high adsorption capacities in the removal of aniline and phenol from a large volume of aqueous
154 solutions, and PANI/MWCNTs can be separated and recovered quickly from solution by a
155 magnet[55]. The authors also claimed that metal and metal oxide-based magnetic materials (such as
156 Fe₃O₄) could be dissolved in acidic solution so that PANI/MWCNTs can be seen as promising material
157 for the separation of organic pollutants from aqueous solutions. Peng et al. used pristine CNTs and
158 graphitized CNTs as an adsorbent to remove 1,2-dichlorobenzene from water. The adsorption is fast,
159 and it takes only 40 min to attain equilibrium. The adsorption capacity of pristine and graphitized
160 CNTs is 30.8 and 28.7 mg/g, respectively. The pristine CNTs are better for adsorption of because they
161 have a rough surface which made adsorption of organic molecules much more accessible[56].

162 Dioxins and related compounds such as polychlorinated dibenzofurans and biphenyls are
163 highly toxic and stable pollutants. Richard Q. Long and Ralph T. Yang found that the interactions of
164 dioxins with CNTs are much stronger than that with activated carbon[57]. Their experimental results
165 show that CNTs are better sorbents for dioxin removal.

166 *Heavy metal ions*

167 Heavy metals include cadmium, chromium, zinc, and lead in water cause serious problem to the
168 environment. CNTs have shown great potential as an attractive adsorbent for the removal of heavy

169 metal ions from contaminated water[58]. The sorption capacities of metal ions by raw CNTs are very
170 low but significantly increase **when** oxidized by HNO₃, NaOCl, and KMnO₄. The adsorption
171 mechanisms are very complicated, and the contributions include physical adsorption, electrostatic
172 attraction, precipitation and chemical interactions [58-60].

173 Chao-Yin Kuo and Han-Yu Lin have researched on the adsorption of aqueous cadmium (II) onto
174 modified multi-walled carbon nanotubes. **They found that** microwave **assistance** involves oxidation
175 **using acids or oxidants**. The research showed that The Cd²⁺ adsorption capacity is increased by
176 modifying the CNTs surfaces. The negatively charged surfaces of modified CNTs electrostatically
177 favored the adsorption of Cd²⁺ in MW/H₂SO₄/ KMnO₄-modified CNTs more than in MW/H₂SO₄-
178 modified CNTs[61]. Ze-Chao Di et. al. developed ceria nanoparticles supported on aligned carbon
179 nanotubes (CeO₂/ACNTs), a novel adsorbent for Cr(VI) from drinking water. The maximum
180 adsorption capacity of CeO₂/ACNTs reaches 30.2 mg g⁻¹ at pH 7.0[62]. Chen et al. modified the surface
181 of MWCNTs with polyacrylic acid and used for the europium adsorption. The incorporation of iron
182 oxide magnetite enhances the separation and recovery after decontamination[63].

183 Several groups did a detailed study on the adsorption of lead ions using MWCNTs. **They**
184 **concluded that** CNTs with a smaller diameter and higher oxygen content show greater lead
185 **adsorption** ability [64,65]. SWCNTs and MWCNTs oxidized by NaClO for nickel removal from
186 aqueous solution was reported by Chungsyng Lu and Chunti Liu[66]. Similarly, HNO₃ oxidized
187 CNTs was used by Changlun Chen and Xiangke Wang[67]. Another NaClO oxidized SWCNTs and
188 MWCNTs used for the zinc **adsorption** was accomplished by Lu et al. Maximum zinc sorption
189 capacity of SWCNTs and MWCNTs calculated by the Langmuir model were 46.94 mg/g and 34.36
190 mg/g, respectively[68,69]. In overall the heavy metal ion **adsorption** by CNTs follow roughly the
191 order: Pb²⁺ > Ni²⁺ > Zn²⁺ > Cu²⁺ > Cd²⁺. The application of CNTs was further extended to decontamination
192 of water from radioactive cesium ions.

193 The sorption capacities by raw CNTs, especially the heavy metal decontamination, are low but
194 significantly increase after functionalization, so most of the **researches** used oxidized CNT. In overall,
195 **CNT is an** excellent material for the remediation of a wide range of organic and inorganic
196 contaminants in contrast to many of the conventional sorbents. Further research on developing cost-
197 effective CNT-related materials are recommended.

198 **Adsorption of cesium and strontium ions**

199 Removal of radioactive cesium and strontium from water has been an unsolved problem until
200 today, being more urgent since the earthquake happened in Japan on March 11, 2011. Fugetsu et al.
201 developed a quaternary spongiform adsorbent that contains Prussian blue, carbon nanotubes,
202 diatomite, and polyurethane, which showed a high capacity for eliminating cesium both in laboratory
203 studies and actual *in situ* Fukushima areas[70]. Low levels of radioactive cesium can be selectively
204 adsorbed from sea water with a portable spongiform adsorbent that **incorporates** Prussian blue as
205 the functional elements, and carbon nanotubes sealed diatomite as the working cavities (Figure 3).
206 Thus-prepared complicated system was then permanently immobilized on the cell walls of
207 polyurethane foam as the matrix. Such quaternary system shows that the elimination efficiency for
208 cesium-137 was 99.93% in deionized water and 99.47% in seawater. Besides this study, Fugetsu group
209 have been spending several years on developing caged approaches to overcome the difficulties
210 associated with colloidal dispersion. We have tested organic polymers (like alginate) and porous
211 inorganic particles (like diatomite) as potential caging materials to fabricate high performance
212 adsorbents [71-77]. We intend to emphasize that highly-dispersed CNTs function not only as effective
213 elements caged in surface negatively-charged gel micro-vesicles accomplished the affinity-based
214 aqueous removal of typical ionic dyes, such as AO, ethidium bromide, eosin bluish and orange G
215 beyond activated carbon and carbon nanofiber [78], but also as nano-thick network leak-proof coating
216 to seal the Prussian blue-carrying-inside diatomite in the polyurethane composite, strengthened the
217 resistance to radioactive irritation, and realized practical capture and transfer of radioactive heavy
218 metal ions, such as cesium [70]. **Previous researches, as mentioned above, having** unveiled carbon
219 **nanotubes were promising** for the purpose of decontamination towards various water-borne dyes
220 and high-risk radioactive dissolved heavy metal ions[70,73,78-82].

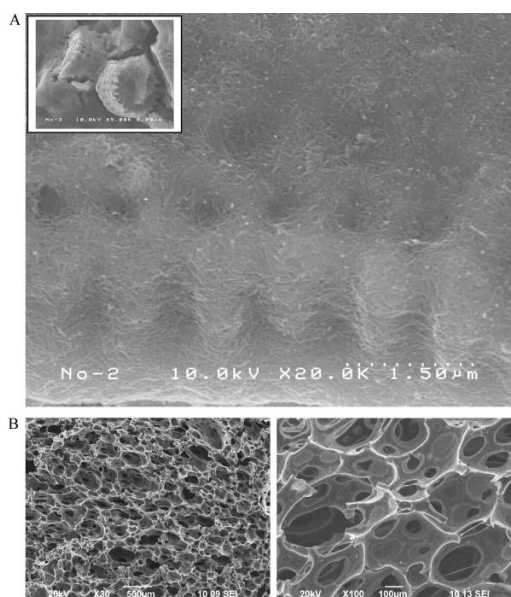


Figure 3. (A) Prussian blue was sealed into the cavities of the diatomite (upper, lower resolution). The diatomite surfaces were coated with highly dispersed multi-walled CNTs (upper, high resolution). The CNTs formed a continuous, interconnected network that prevented the diffusion of Prussian blue particles. (B) Representative SEM images of the quaternary (polyurethane polymer, CNTs, diatomite, and Prussian blue, PUP/CNT/DM/PB), spongiform, Prussian blue based adsorbent. **Reproduced with permission from**[70]. Copyright Elsevier, 2012.

Another kind of portable type of adsorbents (like beads) have been tried to adsorb the cesium ions and strontium ions from contaminated water by Fugetsu et al [80,82]. Prussian blue or its analogues encapsulating alginate beads reinforced with highly dispersed multiwalled carbon nanotubes were used for the studies on the removal mechanism and experimental adsorption of cesium and strontium ions, equipped with comparable kinetics models. Baiyang et al. and Vipin et al. used MWCNTs to enhance the immobilization of Prussian blue nanoparticle in polymeric cages [70,80,82]. They found that CNTs held PB more strongly inside the cage by forming a physical network over PB crystals which enhances the overall performance of adsorbent.

2.2 CNTs in catalysis reaction for water remediation

Photocatalysis

Even today, the wastewater purification is still a theme of large interest[11]. The so-called photocatalytic oxidation/reduction mediated by semiconductors has been discussed as a promising technology for the wastewater treatment in the scientific literature since 1976[83]. Various semiconductor materials such as TiO_2 , Fe_2O_3 , ZnO , etc. have been intensively studied since then [84-87]. However, their quantum efficiency is not high and the speed of ultraviolet photoresponse is not fast. Therefore, the development of modified TiO_2 with enhanced properties is needed to increase the photocatalytic activity for the organic pollutants[88]. Herein, carbon nanotubes are considered to be ideal catalyst carriers as to increase the quantum efficiency and extend the light adsorption region due to their huge specific surface area, remarkable chemical stability, unique electronic structure, nanoscale hollow tube property and good absorbability[27,89-93]. **Herein, we summarized some typical studies of CNTs as catalyst support for water remediation in Table 1.**

250

Table 1. CNTs as catalyst support for water remediation

Materials	Mechanism	Pollutants	Major observations	Ref.
SWCNT/TiO ₂	Photocatalysis	Oil	Antifouling and self-cleaning	[94]
TiO ₂ /SWCNT aerogel	Photocatalysis	MB	High visible light photoactivity	[95]
NCNT/TiO ₂ nanowires	Photocatalysis	MB	High degradation ability and wettability	[96]
MWCNT/TiO ₂	Photocatalysis	MB	High visible light absorbing	[97]
CNT sponge	Electrocatalysis	MB	Continuously high degradation efficiency	[98]
MWCNTs-OH-PbO ₂	Electrocatalysis	Pyridine	High degradation efficiency of pyridine	[99]
CNT thread	Electrocatalysis	Brine	Rapid deionization (2.78 mg g ⁻¹ min ⁻¹)	[100]
MWCNTs-silica aerogel	Adsorption	Oil	Superior oil adsorption capacity, 28.48 cm ³ (oil)/g	[101]
NoCNTs	Catalysis	Phenol	Catalytic activity 57.4 times stronger	[102]

251

252

253

254

255

256

257

258

259

260

261

262

263

264

265

266

267

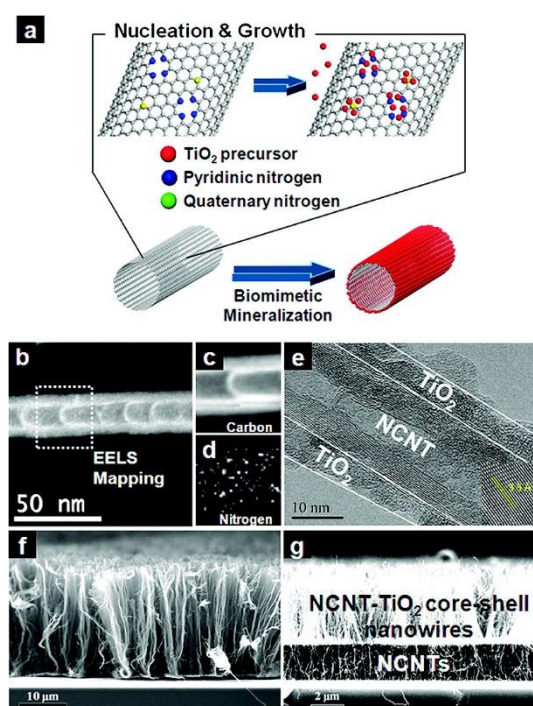
268

269

270

271

Until now, a hybrid of TiO₂ and graphitic carbon (CNT, graphene, etc.) has gained tremendous research interest [103-106]. Ideal TiO₂/graphitic carbon hybrids reinforced with electroconductive and mechanically strong carbon nanotubes or a graphene backbone may possess an extremely large TiO₂/carbon interface that can facilitate electron-hole separation. Moreover, such interfacial hot spots may introduce a new carbon energy level in the TiO₂ band gap and thereby effectively lower the band gap energy [97,107]. Lee et al. have reported the N-doped CNT (NCNT)/TiO₂ core/shell nanowires for visible light-induced MB degradation by biomimetic mineralization of TiO₂ at the graphitic carbon surface [97]. They proposed that N-doped sites on the NCNT attracted Ti precursors and it promoted their condensation to form a highly uniform TiO₂ nanoshell with excellent coverage (Figure 4). Regarding to the NCNT/TiO₂ core/shell nanowires, the biomimetic mineralization yielded highly uniform coverage of a ~5 nm thick TiO₂ nanoshell over the entire length of the vertical CNTs because of the dense evenly distributed N-doping sites. The electroconductive and thermally stable NCNT backbone enabled high temperature treatment that optimized the corresponding crystal structure and properties of TiO₂ nanoshell. The direct contact of the NCNT surface and TiO₂ nanoshell without any adhesive interlayer introduced a new carbon energy level in the TiO₂ band gap, leading to the great visible light photocatalysis in MB degradation. Furthermore, the synergistic properties of core/shell nanowires also greatly enhanced the stimuli-responsive wettability. So this ideal multi-functional TiO₂/graphite-carbon hybrid nanostructure could facilitate a variety of artificial applications, including sensors, catalysts, energy storage and conversion.



272
 273 **Figure 4.** (a) Schematic illustration of biomimetic N-doped CNT (NCNT)/TiO₂ core/shell nanowire
 274 fabrication. Red, blue, and yellow colors indicate TiO₂ precursor, pyridinic N (NP), and quaternary
 275 N (NQ), respectively. N-doping sites act as nucleation sites. (b) ADF-STEM image of NCNT. EELS
 276 mapping shows (c) C and (d) N elements along NCNT. (e) TEM and (f) SEM images of NCNT/TiO₂
 277 core/shell nanowires. The inset shows the lattice distance of the anatase phase. (g) NCNT/TiO₂
 278 core/shell (top) and bare NCNT (bottom) heteronanowires. Reprinted with permission from [97].
 279 Copyright (2012) American Chemical Society.

280 Furthermore, a lot of work are trying to make ultrathin and superwetting membranes to treat
 281 emulsified waste water produced in industry and daily life and also for purification of crude oil and
 282 fuel. Gao et al. reports on the preparation of an ultrathin and flexible film based on an SWCNT/TiO₂
 283 nanocomposite network, with the aid of UV-light irradiation[94]. The ultrathin network film is
 284 superhydrophilic and underwater superoleophobic, so it can effectively separate both surfactant-free
 285 and surfactant-stabilized oil-in-water emulsions with a wide range of droplet sizes (Figure 5). This
 286 robust and flexible SWCNT/TiO₂ nanocomposite films were prepared by coating TiO₂ via the sol-gel
 287 process onto an SWCNT ultrathin network film. The SWCNT/TiO₂ composite network film with
 288 adequate film thickness and nanoscale pore size shows high flux rate about 30000 Lm⁻²h⁻¹bar⁻¹, and
 289 an ultrahigh separation efficiency achieved at 99.99%. Moreover, the characteristic of TiO₂ for
 290 photocatalytic degradation of organic compounds endows the SWCNT/TiO₂ film an excellent
 291 antifouling and self-cleaning properties even after being contaminated with oils. So the SWCNT/TiO₂
 292 for removing oil from oil/water emulsions has potential at industrial scales. Besides, the freestanding
 293 TiO₂/SWCNT aerogel composites that have high visible light photoactivity were reported by
 294 uniformly decorating aerogels of individually dispersed SWCNTs with titania nanoparticles [95].

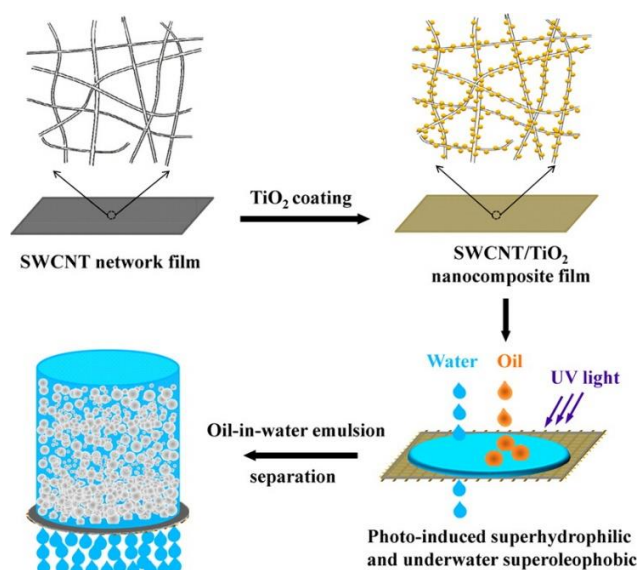


Figure 5. Schematic showing the preparation process of the SWCNT/TiO₂ nanocomposite film and for separation of an oil-in-water emulsion. Reprinted with permission from [94]. Copyright (2014) American Chemical Society.

Electrocatalysis

Electrochemical oxidation is another advanced oxidation process in the treatment of aqueous contaminations. It has attracted much attention because of its automation, fast reaction, environmental compatibility, and safety [108-111]. Some high surface area carbon-based materials such as carbon nanotubes have been extensively used to fabricate composites to adsorb pollutants, which are subsequently degraded by electrochemical oxidation [112,113].

Liu et al. have developed an affordable and effective electrochemical nano-sponge filtration device for water purification applications[98]. The assembly process was first conducted in an aqueous solution of CNTs facilitated by a surfactant, followed by a simple dyeing fabrication process for preparing high-performance conductive nano-sponge electrode. Both carbon nanotubes and polyurethane sponges play important roles in the design of the device. CNTs were incorporated to assist electro-oxidation, which can be used as a highly efficient pollutant degradation electrocatalyst and conductive additive to make polyurethane sponges highly accessible. Polyurethane sponges can be used as a low-cost, porous matrix to effectively carry these carbon nanotube conductors. The as-fabricated gravity fed device could effectively oxidize antibiotic tetracycline (>92%) and methyl orange (>94%) via a single pass through the conductive sponge under the optimized experimental conditions. The as-proposed water treatment technology might be an effective point-of-use device, as well as be scaled up and integrated into current water treatment systems to serve as a polishing step.

As a typical material, PbO₂ has been widely applied in electrochemical oxidation processes and exhibited high electrocatalytic activity[114,115]. In order to improve the oxidation activity of PbO₂ electrodes, Xu et al. prepared MWCNTs-OH-PbO₂ electrodes by adding hydroxyl modified MWCNTs in an electrodeposition solution for electrochemical degradation of pyridine[99]. MWCNTs-OH acted as electron barrier to hinder the successive growth of the big pyramidal PbO₂ particles, then the PbO₂ crystallites grew on the surface of pyramidal PbO₂ particles (Figure 6). This study revealed that the formation of small organic molecules by ring cleavage reaction and direct mineralization to CO₂ and NO₃⁻ might be two potential pathways for electrochemical degradation of pyridine. Moronshing et al. recently reported a scalable approach to achieve efficient water purification by rapid capacitive deionization (CDI) with CNT-thread as electrodes[100]. Due to the synergism between electrical conductivity (~25 S cm⁻¹), high specific surface area (~900 m²g⁻¹), porosity (0.7nm, 3nm) and hydrophilicity (contact angle~25°) in CNT-thread electrode, the extensive electrical double layer will come to rapid formation after contacting with water, and resulting in consequently efficient deionization.

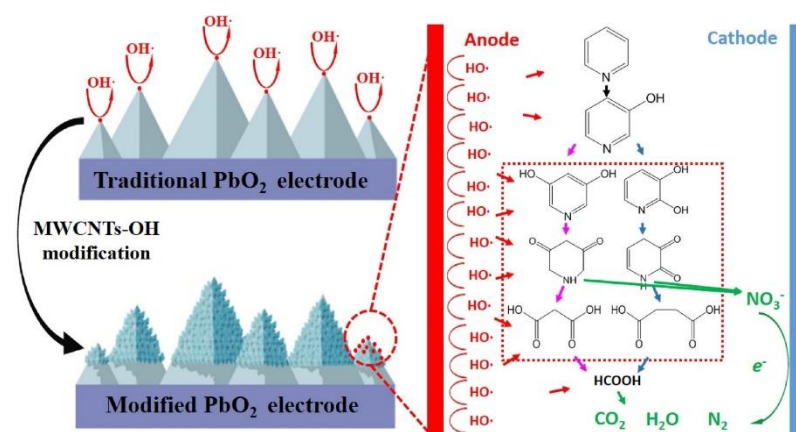


Figure 6. Hydroxyl multi-walled carbon nanotube-modified nanocrystalline PbO₂ anode for removal of pyridine from wastewater. Reproduced with permission from [99]. Copyright Elsevier, 2017.

Other catalytic oxidation

Recently, a novel oxidation technology based on nonradical activation mechanism of peroxydisulfate (PDS) by carbon nanotubes has received increasing attention, showing high reactivity towards phenol, bisphenol A, et al [116,117]. Unlike the case for other advanced oxidation processes in which free radicals are the keys for organic degradation, nonradical processes were also observed on the modified CNT samples upon nitrogen doping. Duan et al. prepared N doped carbon nanotubes (NoCNTs) as metal free catalyst by the chemical modification of SWCNTs with substitutional N incorporation into the rolled graphene sheets for phenol catalytic oxidation[102]. A comprehensive research for the mechanism of peroxymonosulfate (PMS) activation and the roles of nitrogen heteroatoms has been studied. Nitrogen heteroatoms in CNT played a significant role in phenol oxidation with PMS, which might greatly enhance both the radical and nonradical pathways that are beneficial to the phenol degradation. And the nonradical pathway accompanied by radical generation ($\bullet\text{OH}$ and $\text{SO}_4\bullet^-$) enable the NoCNT to have great stability (Figure 7). NoCNT presented an extraordinarily high catalytic activity for phenol removal by PMS activation with a 57.4-fold enhancement over the activity of NoCNT. Thus, this study provided insight to the role of N doped carbon nanotubes for enhanced catalysis and the designing of metal free catalyst with high catalysis performance and stability.

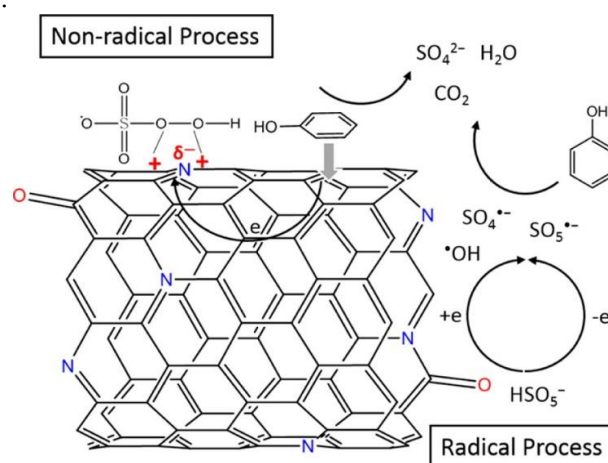


Figure 7. Mechanism of peroxymonosulfate (PMS) activation on N-Doped CNTs. Reprinted with permission from [102]. Copyright (2015) American Chemical Society.

358 3. Graphene oxide (GO) based composite materials for water remediation

359 Adsorption is one of the most important and basic technology as decontamination method. Its
360 dramatic advantages over many other methods include ease of operation and comparatively low cost
361 investment. Adsorption is the surface phenomenon whereby pollutants are adsorbed onto the surface
362 of a material (adsorbent) via physical and/or chemical forces[118,119]. Along with the emergence and
363 bloom of nanotechnologies, applications using carbon nanomaterials have exhibited great promise,
364 especially the graphene derivatives [7,8,23,120-122]. As mentioned above, GO is two-dimension
365 layered structure with large surface area and also rich in various oxygen-containing functionalities
366 which include hydroxyl, carbonyl, carboxylic, and epoxide groups. Therefore, GO is rendered with
367 high water-borne solubility in contrary to graphene, being easily mono-dispersed in the aqueous,
368 unfolding its 2D structure and forming homogeneous colloidal suspension. Moreover, it can
369 positively interact with various pollutants in molecular or ionic forms via the mechanisms, mostly
370 known as the electrostatic interaction, pi-pi interaction, and hydrophobic interaction, etc.[120,121].
371 Therefore, GO has drawn much attention as a nano sized adsorbent [123].

372 Success of a typical adsorption relies on adsorbent providing active sites (imbalanced or residue
373 force at their surfaces) and adsorbate capable of fast migration (Figure 8A). Thus, for activated carbon,
374 the preparation has to go through an extra chemical /physical activation processing besides the
375 carbonization of raw material to generate functioning sites for high performance adsorption. In
376 contrast to bulky status of activated carbon, obtained graphene/GO as above mentioned is in nature
377 of nano sizes, intrinsically with large surface area. Besides, the GO surface-grafted functionalities to
378 large extent help unfold the sheets exposing to foreign contaminants as well as to resist GO's
379 aggregation into flocculates in water, which may have great impact on the utilization performance.

380 As described, GO itself can straightforward act on contaminants, and adsorbs them at an
381 extremely impressive level towards either ions or molecules. In our previous work[120], we selected
382 AO as typical model contaminant. Firstly, it's a practical reagent in the printing and leather
383 industries, and also a versatile fluorescent heterocyclic dye used in the biological research, for
384 example, to observe RNA and DNA in living cells. The exposure to AO may genetically harm living
385 beings as a negative consequence. Secondly, at that time, adsorptive research targeting such kind of
386 dyes with graphene and GO were just a startup field, showing few reports on the influences of GO.
387 And lastly, among those years, we had been paying much attention to carbon nanomaterials,
388 especially the high-dispersion technology (Mono-dispersion Technology) dedicating to extensive
389 applications [75,77], inclusive of environmental restoration, especially the water remediation. In last
390 several years, the community of this field grew so fast that almost instantly graphene/GO had become
391 the celebrities in carbon family. We are also involved in this journey, dedicating to shedding light on
392 the great promise of chemical-exfoliation derived GO, by virtue of our solid nanocarbon research
393 background.

394 3.1 GO as the sole sorbent

395 Table 2 summarizes the researches about the aqueous removal of dyes by GO-related adsorbents
396 mainly in the recent decade. The section "as sole adsorbent" highlights GO itself functioning as the
397 sole adsorbent. Notably, as to preparation of GO, most research referred to modified Hummers
398 methods. As a consequence, there formed a variety of GO adsorbents yet with different terms, for
399 example, GO, sGO, 3D GO_f, GO_p. To some extent, this reflects a little dependence on the raw graphite
400 type, or the expected structure of GO [120,121,124-150].

401 Similarly, highly-dispersed single-layered GO sheets or its derivatives were prepared by
402 ourselves following the Hummers method [124,151,152]. Normally in a complete preparation,
403 centrifugation as well as sonication is conventionally included in purpose of fully exfoliating quasi-
404 stacked graphite oxide. And the sample was traditionally termed as GO. But for discrimination,
405 modification is necessary on naming. Herein, the adsorbent from a modified Hummers' preparation
406 with a 3-cycle sonication and yet without a centrifugation to screening the exfoliated graphite
407 particles, was designated sGO [140]; the GO hydrogel adsorbent with a three dimensional (3D)
408 structure and suffering reduction using sodium ascorbate was named as 3D RGO [131], which in fact

409 was one less oxygenated derivative of GO; the adsorbent GO_p designate to that from the specific
 410 graphite in powder form and the GO_f did from the graphite flakes, while NGO defined the N-doped
 411 GO obtained by adding melamine of fixed amounts when the preparation of GO underwent [153];
 412 the adsorbents GO-AG,FG,LG,VG were respectively used to describe GO from graphite with
 413 different graphitization degrees [142]. In general, GO can be facily prepared via the Hummers
 414 method or other modified ways. However, through the same procedure, different groups including
 415 us can hardly assure the resultant GO sheets of each time being of absolutely identical characters due
 416 to the difference in terms of the types of graphite, some operational steps and/or the on-purpose
 417 treatment of structures. As to conducting the same research by different groups, the experiment is
 418 unavoidable to suffer from a big variation due to additional subjective factors, such as what graphite
 419 to choose, what modified Hummer method to use and so on. Thus, GO itself as adsorbent may
 420 already have non-negligible structural differences. This to a large extent explained the discrepancies
 421 of adsorptive performances in regard to the capacity (from thousands of microgram dye mass per
 422 gram GO mass to tens of), isotherms and kinetics, as shown in the Table 2.

Table 2. A summary of dye removal by GO materials

Adsorbents	Dye	Isotherm type	Experiment (Calculation) mg g ⁻¹	Kinetic type	Ref.				
GO [#]	MB	Langmuir	220(351)	-	[146]				
	MG		180(248)						
HmGO [#]	MB	Freundlich	387.9	PSO	[144]				
GO [#]	MB	-	199.2*	PSO	[145]				
	RhB		154.8*						
	CV		195.4*						
GO SRGO	AO	Langmuir	1382 (1428) 2158 (3333)	-	[120]				
GO sponge	MB	-	389	PSO	[132]				
	MV		385.7						
sGO	AO	-	94.6	PSO	[140]				
	MB		123.3						
	CV		125.0						
GO	AO	-	229.8	-	[154]				
GO	AO8	Langmuir	25.6(29)	PSO	[125]				
	DR23		14.0(15.3)	PSO					
GO	BR12	Langmuir	(63.69)	-	[126]				
	MO		(16.83)	-					
GO AC CNTs	MB	Langmuir	240.65(243.9) 263.49(270.27) 176.02(188.68)	PSO PSO PSO	[130]				
3D RGO	MB	Freundlich	6.17*	PSO	[131]				
	RhB		9.18*						
GO	MB	Langmuir	(286.9)	PSO	[155]				
GO _p			(12.56)						
NGO _p -1wt%			(11.06)						
NGO _p -2wt%			(16.84)						
NGO _p -3wt%	CR	Langmuir	(19.49)	PSO	[153]				
GO _f			(12.42)						
NGO _f -1wt%			(9.59)						
NGO _f -2wt%			(11.64)						
NGO _f -3wt%			(14.17)						
GO-VG			CB			Langmuir	3071.47(3206.66)	PSO	[142]
GO-LG							3261.25(3414.92)		

As Sole adsorbent

	GO-FG			3404.80(3587.92)		
	GO-AG			3953.92(4248.79)		
	GO	MB	Langmuir	927(476.19)	PSO	[143]
		BG		724(416.67)		
	GO	MB	-	-	-	[149]
As Composite element	SA-GO-N	AO	Langmuir	797(836)	PFS	[121]
	SA-GO-M	AO	Langmuir	1351(1420)	PFS	[121]
	RL-GO	MB _{ch}	BET,Freundli	(309)	PSO	[128]
	KGM	MO	Freundlich	51.6	PSO	[139]
		MB		92.3		
	5wt%GO CB	MG	Langmuir	(17.862)	PSO	[150]
	MGSi	AO	Freundlich	-	PSO	[156]
	LI-MGO	AO	Langmuir	62.08 (132.80)	PSO	[135]
		CV		37.88(69.44)		
		OIV		39.46(57.37)		
		GR		147.8(588.24)		
	GO-LCTS	MB	Langmuir	(402.6)	PSO	[155]
GO/1-OA	MG	Freundlich	2687.56	PSO	[134]	
	ER		1189.1			
polyHIPEs/GO	MB	-	1250.3*	PSO	[133]	
	RhB		1051.1*			

Note: - means the publication does not note; * the data is predicted by a kinetic model simulation; # the term GO used here indicates graphite oxide, but its preparation in fact followed the same Hummers method as those without this tag; RT means room temperature.

Most of the adsorptions of dyes onto sole GO agreed well with the Langmuir isotherm and followed the PSO kinetic model. In the early decade, only few reports discussed about nanocarbons in application of conventional dye removal since the high-cost disadvantage. As one early research, Bradder et al. [146] applied incomplete exfoliation form of GO (graphite oxide prepared by a modified Hummers method without post sonication) as an adsorbent for the removal of MB and MG from the aqueous. In contrast to graphite, they found the surface area of GO got little increased, while to the adsorption its surface oxygen functional groups played significantly important role. Intrinsic electrostatic attraction between GO and dyes resulted in a higher amount of the dyes adsorbed on the GO, and meanwhile a Langmuir-type monolayer isotherm.

To dig the superiority of merged carbonaceous nanomaterials, Li et al. (2013) [130] conducted the adsorptions of MB with nitric acid-treated carbonaceous materials, namely GO, activated carbon(AC) and CNTs. Due to the pi-pi electron donor-acceptor interaction and electrostatic attraction mechanism, all the adsorptions took on a Langmuir monolayer behavior with a pseudo second-order kinetic process. Differing in surface area accessibility, GO won CNTs and AC with the larger adsorption capacity normalized by the BET surface area.

Ghaedi et al. [143] researched the mixed adsorption of cationic dyes (MB and BG) by the GO prepared from a pre-oxidation-involved modified Hummers method. They found both the MB and BG removal were in a PSO kinetic process following a monolayer manner. They attributed the mechanism closely relative to the large surface area combining with the pi-pi electron donor acceptor interactions and electrostatic attraction between positively charged dye ions and negatively charged GO. Keeping searching more efficient adsorbents, Robati et al. [126] used commodity GO (atomic layer - at least 80%). It could remove the cationic BR12 and anionic MO within ~100 min from the aqueous at a pH ~3. It was found with the Langmuir monolayer adsorptive behavior through endothermic process. Interestingly, they observed the initial concentration of dyes affected oppositely on final adsorption capacity, namely an increase for the cationic BR12 while a decrease for the anionic MO if the initial dye amount increased.

453 Specifically to the anionic dyes, Konicki et al. [125] selected AO8 and DR23 as adsorbate for
454 testing GO. Excluding hydrogen bonding, AO8 and DR23 are non-planar molecule hardly attaching
455 to the skeleton of GO via formation of pi-pi stacking interactions due to spatial restriction, and thus,
456 electrostatic attraction was probably the major contribution to the mechanism. As a result, the
457 adsorptions presented more of a Langmuir model behavior than the R-P model and underwent in a
458 PSO kinetic way. Meanwhile in another group, Jiao et al. [142] investigated the cationic blue with GO
459 synthesized from four kinds of graphite with different graphitization degrees, designated as GO-AG
460 (C/O ratio: 55.97), GO-FG (61.48), GO-LG (71.43), GO-VG (75.78). Likewise, all adsorptions came up
461 with the same conclusion. Besides, highly disordered graphite (lower C/O) favored both the
462 preparation and the adsorption capacity of GO. More and more recently, doping method emerged
463 and endowed GO with more potential in water treatment. For instance, Yokwana et al. [85] prepared
464 nitrogen-doped GO nano-sheets (NGO) using either graphite powder (NGO_p) or graphite flakes
465 (NGO_f). The removal of the CR could achieve a maximum efficiency of 98%~99% for NGO_p and
466 96%~98% for NGO_f at the pH of 2. As concluded, there existed electrostatic interactions between the
467 negatively charged (oxygen-containing) and positively charged (nitrogen-containing) groups on the
468 NGO and the positively charged (amino and cationic azo-linkages) and negatively charged (sulfonic
469 (SO₃⁻) groups on the anionic CR dye molecules, possibly leading to the monolayer and PSO
470 adsorptions.

471 From the perspective of GO, Sabzevari et al. [155] found GO prepared without sonication with
472 the purpose of the removal of the cationic MB even suggested a relatively high monolayer uptake
473 and took a PSO kinetic profile. More interestingly, He et al. [144] found their HmGO [157] prepared
474 with no sonication too, led to the highest adsorption capacity for MB in comparison to other GO with
475 sonication or from original Hummers method [158]. They found expansion of lamellar spacing,
476 maintenance of lamellar structure and negatively charged oxygen-containing groups were favorable
477 for the adsorption. The GO-MB chemical interactions led to the adsorption with a PSO kinetic process.
478 A little earlier, Jin et al. [145] investigated the removal of cationic MB, CV and RhB dyes with the
479 graphite oxide prepared by a modified Hummers method in which conventional mid- plus high-
480 temperature reactions replaced a 12-hrs 70-°C sealed autoclave reaction. They speculated the dye
481 molecules probably appeared in a head-to-tail form of aggregation when adsorbed in the layered
482 structure, thus to some extent leading to different multilayer adsorption. With the chemical sorption
483 nature, the adsorption still showed a PSO kinetic process.

484 It is worth of noticing that due to the homogeneity and large surface area, fully exfoliated,
485 namely, single-layered GO could reach extremely high adsorption capacity. [120,134] However, the
486 recovery of GO adsorbent becomes tedious and cost due to the operation inescapable of a prolonged
487 ultrahigh centrifugation. To change the situation, a centrifugal vacuum evaporation method
488 proposed by Liu et al. [159] was used to generate 3D GO sponges from suspensions and the sponges
489 successfully removed over 98% of the MB and MV in two minutes, reflecting high capacity and fast
490 rate. It was pointed out that the endothermic chemical adsorption mechanistically replied on the
491 strong pi-pi stacking and anion-cation interaction with the activation energy of 50.3 and 70.9 kJ mol⁻¹.
492 Tiwari et al. [131] synthesized uniformly mesoporous 3D RGO hydrogels by the reduction of a
493 mixture of mono-, bi-, and tri-layer graphene oxides with large surface area using sodium ascorbate
494 and simultaneous gelation. For the adsorption, they found such pi-pi stacking and anion-cation
495 interactions dominated the mechanism, yet resulting in a Freundlich-type multi-layer adsorptive
496 behavior with high removal capabilities for MB (100%) and RhB (97%) under initial concentrations of
497 ~0.6 g L⁻¹.

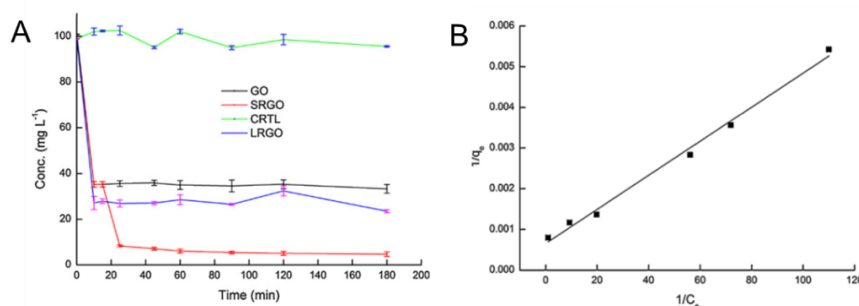
498 In fact, GO was rather seldom studied to remove AO, unlike MB, MO, RhB etc. Only a few
499 published contributions were found. Coello-Fiallos et al. [154] investigated the dye removal by the
500 GO from natural graphite by modified Hummer's method. By analyzing the changes in the stretching
501 vibrational bands of C-N and C-C, chemical interaction was corroborated between the AO and the
502 functional groups of GO. The adsorptive equilibrium was found acquired within 1 hour with 40%
503 removal efficiency. Afterwards, Coello-Fiallos et al. [140] continued the targeted study, including dye
504 AO, with sonicated graphite oxide (sGO) prepared without centrifugation. Again, GO chemically

505 adsorbed the cationic dyes AO more beyond CV and MB, and the processes followed the PSO model.
 506 Interestingly, Liu et al. [149] taking GO as a flocculant, observed that it could fast remove nearly all
 507 the MB from the aqueous and concluded that the MB cations were attracted by GO through the Van
 508 de Waals mechanism, other than frequently-reported electrostatic interaction as predicted by PIXEL
 509 energy contribution analysis in their research, and quickly congregated around GO in water. These
 510 conflicting mechanisms suggested further studies remain necessary, especially with multiple visual
 511 angles.

512 Prior to them, we ourselves targeted AO as a model contaminant. Through the simple adsorbent-
 513 adsorbate adsorption (Figure 8A, Figure 9A black line), a visible change of solution in color was
 514 obtained once the GO was added and demonstrated well elimination of AO from the aqueous phase.
 515 Likewise, modeling studies indicated all adsorptions behaved in a Langmuir-type monolayer
 516 manner. GO was found to have a maximal capacity of over 1400 mg g⁻¹, a record performance at that
 517 time. Even now, this is still remarkable as compared in the Table 2 [120]. At the same time, we noticed
 518 that all above researches were categorized as conventional one-step adsorption study, the final
 519 performance highly depended on the already-have functionalities or structures of the adsorbent,
 520 despite whether they are adsorption reactive or not. For full utilization of the 2D structure, we
 521 proposed a two-step adsorption (Figure 8B), of which GO was termed as SRGO (Figure 9A red line).
 522 The enhancement was realized via an additional in-situ slight chemical reduction to the GO that had
 523 reached the first equilibrium in the one-step adsorption. Amazingly, the transforming of its surface
 524 groups to more hydrogen-bonding active sites (pH<7) resulted in a remarkable increase of GO
 525 capability over 3000 mg g⁻¹ (Figure 9A red line), highlighting an extraordinary performance than GO
 526 itself. Meanwhile, such a two-step method did not alter the monolayer adsorptive manner (Figure
 527 9B, Langmuir fitting). Importantly, this novel modification is of high repeatability, promising for
 528 emergency handling, which still pushing our team forward for more practical scenarios.



529
 530 **Figure 8.** (A) The schematic diagram of conventional one-step adsorption; (B) Enhanced two-step
 531 adsorption: simultaneously generate new sites from inactive structures for enhanced capacity.



532
 533 **Figure 9.** (A) Time-dependent adsorption of dye acridine orange by GO, in-situ reduced GO (SRGO),
 534 three-hour-long pre-reduced GO (LRGO) versus the blank group, AO ~100 mg/L, 50 ml; (B)
 535 Adsorption isotherms fitted by the Langmuir model: the reciprocal of equilibrium concentration
 536 versus that of equilibrium capacity. Adapted with permission from [120]. Copyright Elsevier, 2012.

537 3.2 GO as composited element

538 The section “as composite element” of the Table 2 summarizes some recent work using GO-
 539 composited adsorbents for typical dye removal. Notably, to the same purpose, GO-composited
 540 catalysts were also investigated. Frankly speaking, straightforward utilization of GO as the sole
 541 adsorbent still faces some problems, like inconvenient recovery and recycle, potential environment
 542 risk coming from its biotoxicity, and so on. To these ends, host materials were applied to composite
 543 GO inside. In the coming researches, main origins of novelty came from the merits inclusive of green

544 preparation, high capacity, easy separation, recycle availability, etc. As a matter of fact, GO exhibited
545 great potentials in an extensive scope for environmental applications and also such guest-host
546 composites still suggested superiorities concerning the adsorptive capacity, batch kinetics and other
547 indicators.

548 *Surface functionalization: GO as host material*

549 Conventional functionalization potentially risks from the fall-off of the loading materials from
550 the host, influencing the working lifespan. To this end, Wang et al. [156] adopted a modified two-
551 phase co-precipitation method and synthesized a magnetic calcium silicate graphene oxide
552 composite adsorbent (MG) with improved joint stability. Consequently, such composite had
553 selectivity of adsorption targeting AO other than CV and MB, ascribed to the higher electropositivity
554 of AO in comparison to that of MB and less steric hindrance than the CV. The adsorption followed a
555 pseudo-second-order kinetic model and yet in a Freundlich-type multi-layer manner. Wu et al. [128]
556 examined a rhamnolipid-functionalized graphene oxide (RL-GO) composite prepared in one-step
557 ultra-sonication as a cost-effective sorbent for artificial and real MB wastewater treatment. It
558 contained abundant functional groups and a mesoporous structure and was insensitive to ionic
559 strength variation when adsorption proceeded. It spontaneously and endothermically adsorbed the
560 MB in a PSO and multilayer adsorptive manner (better fitting by both BET and Freundlich models),
561 resulting from the synergetic mechanism of electrostatic attraction, pi-pi interaction and hydrogen
562 bonding interactions.

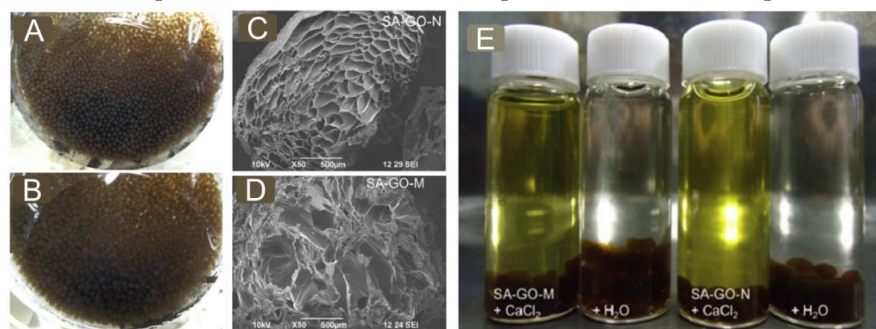
563 Small organic molecules functionalized GO via non-covalent interactions are rarely explored for
564 environmental remediation, due to the lack of stability in water of the resultant material though it is
565 more versatile than covalent modification. Note that the 1-OA composite was formed from tetrazolyl
566 compound 1 (1, 3-di(1H-tetrazol-5-yl) benzene) and octadecylamine (OA), having cooperative non-
567 covalent forces to co-adsorb dyes and metal ions. Lv (2018) [134] brought this idea as reported into
568 fabricating a two-component supramolecular 1-OA functionalized GO. As a consequence, in addition
569 to easy solid-liquid separation and simple recycle, the modified GO/1-OA displayed a remarkable
570 adsorption performance for pollutant dyes, BPA (endocrine-disruptor), Ciprofloxacin
571 (pharmaceutical) and Cu^{2+} in the single system or in their binary, ternary and quaternary pollutant
572 mixtures. In the case of the cationic MG and anionic ER removal, the adsorptions suggested superior
573 capabilities following the PSO kinetic mode and in a multilayer adsorptive behavior. Learned from
574 these examples, we understood functionalization of GO would not weaken the whole removal
575 efficiency for adsorbent but even got further enhancement. On the other hand, structure fragility
576 remains as a fact what we worried about.

577 *Crosslinking: GO in host materials*

578 Several advantages of this strategy make it especially attractive. First, the fabrication goes always
579 with a relatively simple and non-toxic route. Second, the adsorbent shows stable structure
580 configuration and good adsorptive performances. Third, the adsorbent can be easily isolated by hand
581 from the targeted solution and regenerated by some simple methods, for example, re-immersing in
582 reactive solution [160], such as Ca^{2+} , H^+ and so on.

583 From this point of view, polysaccharides are commonly seen as green and economic biomaterials
584 around us, including alginate, cellulose, chitosan and so on. With targeting the removal of AO and
585 considering the porosity enrichment by **inserting GO into many other matrices, we prepared GO**
586 **homogeneously-loaded millimeter-sized beads (Figure 10A-D) [121]** with biocompatible sodium
587 alginate cross-linked by either Ca^{2+} or H^+ . These beads were characterized with a remarkable increase
588 in pore structure and therefore exposed more functioning sites; in other word, they possessed better
589 performances by contrast to that of those references. The ion exchange (Figure 10E) based electrostatic
590 interactions as the main mechanism was found to play a vital role and led to the Langmuir-type
591 adsorption. But we found the adsorptive processes were consistent with the non-linearized PFO
592 model. Similarly, Zhang et al. [150] reported GO was fully blended into cellulose matrix and
593 subsequently cross-linked to form the GO/CB composites. The removal processes behaved in the
594 Langmuir-type manner and PSO kinetic model. Integrating the merits of the GO and cellulose, the

595 composites turned out with high removal efficiency (MG, >96%) and easy reusability (>5 times),
 596 strongly dependent on encapsulation amount of GO, temperature and solution pH.



597
 598 **Figure 10.** (A) Ca^{2+} cross-linked GO-alginate composite beads (SA-GO-N); (B) Acid-gelled GO-alginate
 599 composite beads (SA-GO-M); (C) a SEM image of freezing-dry bead SA-GO-N; (D) a SEM image of
 600 the bead SA-GO-M; (E) naked-eye comparison of color changes upon dye-adsorbing beads (SA-GO-
 601 M and SA-GO-N) were immersed in the CaCl_2 ~0.5 mol/L solution and deionized water. Adapted
 602 with permission from [121]. Copyright Elsevier, 2014.

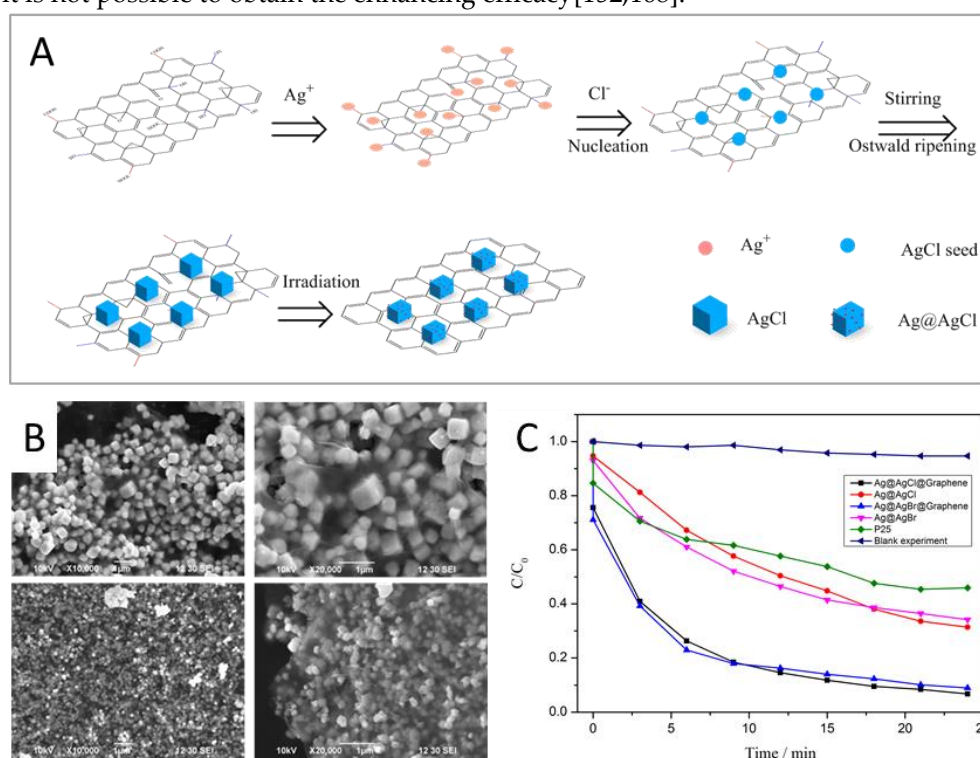
603 Gan et al. presented a konjac glucomannan (KGM) as GO matrix, and prepared GO/KGM based
 604 calcium oxide cross-linked hydrogel adsorbent to adsorb MO and MB[139]. Likewise, the presence
 605 of GO endowed the hydrogel adsorbent with enhanced adsorbing performance compared to neat
 606 KGM hydrogel. And the adsorption followed a PSO kinetics and Freundlich-type multilayered
 607 model. Recently, Sabzevari et al. [155] pointed out that current GO framework products were of
 608 limited applications in water treatment because of scalability as the result of repulsive hydration
 609 forces between GO layers. To this end, they tried to cross-link GO within chitosan to yield a composite
 610 (GO-LCTS) via the interaction between the amine groups of chitosan and the carboxyl groups of GO,
 611 resulting in enhanced surface area and structural stability. Such changes and the variable
 612 morphology of GO-LCTS (402.6 mg g^{-1}) were proved to uptake more MB over pristine GO (286.9 mg g^{-1})
 613 and in a Langmuir-type adsorption behavior.

614 In addition to the natural biomaterials, polymer materials are also readily available for this
 615 purpose. Actually, the use of polymers to immobilize GO could even allow unique properties for
 616 solid phase separation and adsorption as the examples. Huang et al. [133] developed a
 617 hypercrosslinked porous polymer monolith adsorbent (polyHIPEs/GO) by modifying the GO with
 618 PVP and then hybridizing such nanocomposite into polymeric high internal phase emulsions (HIPEs)
 619 further with a high temperature polymerization. Its adsorptions towards cationic MB and RB
 620 complied with PSO kinetic model. A further amination of polyHIPEs/GO realized the anionic dye
 621 removal, and such composite turned out with a largely improved adsorption capacity $\sim 1967.3 \text{ g g}^{-1}$
 622 on the model dye eosin Y. They also noticed that increasing GO in quantity can enhance to some
 623 extent both the electrostatic interaction and pi-pi interaction, resulting in a higher uptake of cationic
 624 and anionic dyes. From these studies we found even though GO is faded to a minor component of an
 625 adsorbent, its naturally occurring multiple interactions with target pollutants still exist and moreover,
 626 the aspect of content ratio still influences the final performance of composite adsorbents.

627 *Morphology-controlled composites: GO as the catalysts template*

628 In addition to the direct adsorption effect on the various contaminants, the emergence of GO has
 629 received extensive attention and shows great potential as additional yet determinative
 630 agent/template in the formation of photocatalyst single crystals. During this process, GO can
 631 selectively control the growth direction of inorganic nanoparticles owing to the intrinsic hydroxyl,
 632 epoxy and carboxylic functional groups, which could act as active anchoring sites for the
 633 heterogeneous nucleation of metal ions such as Au^{3+} , Ag^+ , Ti^{3+} , Zn^{2+} , Ca^{2+} , etc.[161-163]. Wang et al.
 634 prepared new cubic $\text{Ag}@\text{AgX}@\text{Graphene}$ ($\text{X} = \text{Cl}, \text{Br}$) nanocomposites by a GO sheet-assisted
 635 assembly protocol, where GO sheets act as a novel amphiphilic template for hetero-growth of AgX
 636 nanoparticles (Figure 11 A). Morphology transformation of AgX nanoparticles from sphere to cube-
 637 like shapes was accomplished by involving GO (Figure 11 B). Functional groups containing the
 638 hydroxyl, epoxy and carboxylic groups could act as active anchoring sites for heterogeneous

639 nucleation of Ag^+ ions [164]. The resultant cubic Ag@AgX@Graphene ($X = \text{Cl}, \text{Br}$) nanocomposites
 640 exhibit enhanced adsorption capacity, and reinforced electron-hole pair separation in the
 641 decomposition of AO dye (Figure 11 C). After that, tetrahedral Ag_3PO_4 crystals with morphology
 642 transformation from rhombic dodecahedrons has been also confirmed by the hybridization with GO
 643 sheets [165]. GO incorporated polymers such as poly (vinyl alcohol) (PVA) has been studied by our
 644 group. The role of GO contribute not only the enhancing the mechanical properties but also adjusting
 645 the morphology and the porous structure [166,167]. During the hybridization, GO or graphene for
 646 this kind of photocatalyst needs to be arranged in a single-layered and/or few-layered manner,
 647 otherwise it is not possible to obtain the enhancing efficacy [152,168].



648 **Figure 11.** Schematic explanation for morphology evolution of the representative
 649 Ag@AgCl@Graphene nanocomposites (A). SEM images of the as-prepared cubic Ag@AgCl and
 650 quasi-cubic Ag@AgBr nanoparticles encapsulated by gauze-like graphene sheets in
 651 Ag@AgCl@Graphene (B, upper) and Ag@AgBr@Graphene (B, lower), respectively. Photocatalytic
 652 performance of the thus-prepared Ag@AgX@Graphene plasmonic photocatalysts for the degradation
 653 of the AO pollutant under sunlight irradiation (C). Reproduced with permission from [164].
 654 Copyright Royal Society of Chemistry, 2013.

656 4. Prospective outlooks and conclusions

657 In spite of the enormous progress already achieved in preparation, composited processing and
 658 applications of the low-dimensional carbon nanomaterials e.g. carbon nanotubes, graphene oxide
 659 and its derivatives within the areas of environmental remediation, challenges and opportunities in
 660 practical application remain to be created and grasped. Although many technologies highlighted in
 661 this review are still in laboratory level, some of them have undertaken to begin the in-situ tests or
 662 even prepared for the commercialization. Among them, adsorption or integrated adsorption-
 663 catalysis system would be the most promising way in full scale application based on the cost-
 664 effectiveness, safety and operability of carbon nanomaterials. We can anticipate that more research
 665 results in laboratory level can be applied into the real solutions through collaborations in terms of
 666 research groups and scientific facilities.

667 Multiple adsorption mechanisms are acting simultaneously on the surface of both CNTs and
 668 GO. The mechanism is always complicated and sometimes variable in accordance with the changes
 669 of surface functionalization and environmental test conditions. Meanwhile, the catalysis or catalysis

670 support role of CNTs and GO needs to be studied deeply in the future. Constructions of effective
671 adsorption-catalysis integrative systems are appreciated with the aid of template effect of CNTs and
672 GO nanosheets. It is our faith that technologies involved with novel materials and science will
673 eventually solve the environment and energy problems and bring a sustainable world for all in the
674 near future.

675 **Author Contributions:** Writing-Review & Editing, Y.Q.W., C.P., A.K.V., L.S., W.C.; Editing & Supervision,
676 Y.Q.W.

677 **Funding:** Y.Q.W. thanks the support from Nihon Trim Co. Ltd. L.S. thanks the support from Beijing University
678 of Technology (105000546317502, 105000514116002) and Beijing Municipal Education Commission
679 (KM201910005007). W.C. thanks the support from National Science Foundation of China (NSFC) # 21872098.

680 **Acknowledgments:** Y.Q.W. thanks Prof. Bunshi Fugetsu for his advice.

681 **Conflicts of Interest:** The authors declare no conflict of interest. The founding sponsors had no role in the design
682 of the study; in the collection, analyses, or interpretation of data; in the writing of the manuscript, and in the
683 decision to publish the results.

684 References

- 685 1. Shannon, M.A.; Bohn, P.W.; Elimelech, M.; Georgiadis, J.G.; Mariñas, B.J.; Mayes, A.M. Science and
686 technology for water purification in the coming decades. *Nature* **2008**, *452*, 301.
- 687 2. Elimelech, M.; Phillip, W.A. The future of seawater desalination: Energy, technology, and the environment.
688 *Science* **2011**, *333*, 712-717.
- 689 3. Werber, J.R.; Osuji, C.O.; Elimelech, M. Materials for next-generation desalination and water purification
690 membranes. *Nature Reviews Materials* **2016**, *1*, 16018.
- 691 4. Ma, L.; Dong, X.; Chen, M.; Zhu, L.; Wang, C.; Yang, F.; Dong, Y. Fabrication and water treatment
692 application of carbon nanotubes (cnts)-based composite membranes: A review. *Membranes* **2017**, *7*, 16.
- 693 5. Hamasaki, T.; Harada, G.; Nakamichi, N.; Kabayama, S.; Teruya, K.; Fugetsu, B.; Gong, W.; Sakata, I.;
694 Shirahata, S. Electrochemically reduced water exerts superior reactive oxygen species scavenging activity
695 in ht1080 cells than the equivalent level of hydrogen-dissolved water. *Plos One* **2017**, *12*, e0171192.
- 696 6. Nakayama, M.; Kabayama, S.; Ito, S. The hydrogen molecule as antioxidant therapy: Clinical application
697 in hemodialysis and perspectives. *Renal Replacement Therapy* **2016**, *2*, 23.
- 698 7. Khan, S.T.; Malik, A. Engineered nanomaterials for water decontamination and purification: From lab to
699 products. *Journal of hazardous materials* **2019**, *363*, 295-308.
- 700 8. Kyzas, G.Z.; Deliyanni, E.A.; Bikiaris, D.N.; Mitropoulos, A.C. Graphene composites as dye adsorbents:
701 Review. *Chemical Engineering Research & Design* **2018**, *129*, 75-88.
- 702 9. De Volder, M.F.L.; Tawfick, S.H.; Baughman, R.H.; Hart, A.J. Carbon nanotubes: Present and future
703 commercial applications. *Science* **2013**, *339*, 535-539.
- 704 10. Mauter, M.S.; Elimelech, M. Environmental applications of carbon-based nanomaterials. *Environmental*
705 *Science & Technology* **2008**, *42*, 5843-5859.
- 706 11. Qu, X.; Alvarez, P.J.J.; Li, Q. Applications of nanotechnology in water and wastewater treatment. *Water*
707 *Research* **2013**, *47*, 3931-3946.
- 708 12. Goh, K.; Chen, Y. Controlling water transport in carbon nanotubes. *Nano Today* **2017**, *14*, 13-15.
- 709 13. Gupta, V.K.; Kumar, R.; Nayak, A.; Saleh, T.A.; Barakat, M.A. Adsorptive removal of dyes from aqueous
710 solution onto carbon nanotubes: A review. *Advances in Colloid and Interface Science* **2013**, *193-194*, 24-34.
- 711 14. Feicht, P.; Eigler, S. Defects in graphene oxide as structural motifs. *ChemNanoMat* **2018**, *4*, 244-252.
- 712 15. Brodie, B.C. On the atomic weight of graphite. *Philosophical transactions of the royal society of London* **1859**,
713 *149*, 249-259.
- 714 16. Boehm, H.P.; Setton, R.; Stumpp, E. Nomenclature and terminology of graphite intercalation compounds.
715 *CARBON* **1986**, *24*, 241-245.
- 716 17. Balandin, A.A.; Ghosh, S.; Bao, W.; Calizo, I.; Teweldebrhan, D.; Miao, F.; Lau, C.N. Superior thermal
717 conductivity of single-layer graphene. *Nano letters* **2008**, *8*, 902-907.
- 718 18. Geim, A.K. Graphene: Status and prospects. *Science (New York, N.Y.)* **2009**, *324*, 1530-1534.
- 719 19. Li, Y.; Wang, X.; Wang, W.; Qin, R.; Lai, W.; Ou, A.; Liu, Y.; Liu, X. Nitrogen-doping chemical behavior of
720 graphene materials with assistance of defluorination. *The Journal of Physical Chemistry C* **2019**, *123*, 584-592.

- 721 20. Padmajan Sasikala, S.; Lim, J.; Kim, I.H.; Jung, H.J.; Yun, T.; Han, T.H.; Kim, S.O. Graphene oxide liquid
722 crystals: A frontier 2d soft material for graphene-based functional materials. *Chemical Society reviews* **2018**,
723 *47*, 6013–6045.
- 724 21. Dreyer, D.R.; Park, S.; Bielawski, C.W.; Ruoff, R.S. The chemistry of graphene oxide. *Chemical Society reviews*
725 **2010**, *39*, 228–240.
- 726 22. Wei, L.; Karahan, H.E.; Zhai, S.; Liu, H.; Chen, X.; Zhou, Z.; Lei, Y.; Liu, Z.; Chen, Y. Amorphous bimetallic
727 oxide–graphene hybrids as bifunctional oxygen electrocatalysts for rechargeable zn–air batteries. *Advanced*
728 *Materials* **2017**, *29*, 1701410.
- 729 23. Lim, J.Y.; Mubarak, N.M.; Abdullah, E.C.; Nizamuddin, S.; Khalid, M.; Inamuddin. Recent trends in the
730 synthesis of graphene and graphene oxide based nanomaterials for removal of heavy metals - a review.
731 *JOURNAL OF INDUSTRIAL AND ENGINEERING CHEMISTRY* **2018**, *66*, 29–44.
- 732 24. Sarkar, B.; Mandal, S.; Tsang, Y.F.; Kumar, P.; Kim, K.-H.; Ok, Y.S. Designer carbon nanotubes for
733 contaminant removal in water and wastewater: A critical review. *Science of The Total Environment* **2018**, *612*,
734 561-581.
- 735 25. Muhulet, A.; Miculescu, F.; Voicu, S.I.; Schütt, F.; Thakur, V.K.; Mishra, Y.K. Fundamentals and scopes of
736 doped carbon nanotubes towards energy and biosensing applications. *Materials Today Energy* **2018**, *9*, 154-
737 186.
- 738 26. Das, R.; Leo, B.F.; Murphy, F. The toxic truth about carbon nanotubes in water purification: A perspective
739 view. *Nanoscale Research Letters* **2018**, *13*, 183.
- 740 27. Yan, Y.; Miao, J.; Yang, Z.; Xiao, F.-X.; Yang, H.B.; Liu, B.; Yang, Y. Carbon nanotube catalysts: Recent
741 advances in synthesis, characterization and applications. *Chemical Society Reviews* **2015**, *44*, 3295-3346.
- 742 28. Das, R.; Abd Hamid, S.B.; Ali, M.E.; Ismail, A.F.; Annuar, M.S.M.; Ramakrishna, S. Multifunctional carbon
743 nanotubes in water treatment: The present, past and future. *Desalination* **2014**, *354*, 160-179.
- 744 29. Liu, X.; Wang, M.; Zhang, S.; Pan, B. Application potential of carbon nanotubes in water treatment: A
745 review. *Journal of Environmental Sciences* **2013**, *25*, 1263-1280.
- 746 30. Varghese, S.S.; Lonkar, S.; Singh, K.K.; Swaminathan, S.; Abdala, A. Recent advances in graphene based
747 gas sensors. *Sensors and Actuators B: Chemical* **2015**, *218*, 160-183.
- 748 31. Yuan, W.; Shi, G. Graphene-based gas sensors. *Journal of Materials Chemistry A* **2013**, *1*, 10078-10091.
- 749 32. Kemp, K.C.; Seema, H.; Saleh, M.; Le, N.H.; Mahesh, K.; Chandra, V.; Kim, K.S. Environmental applications
750 using graphene composites: Water remediation and gas adsorption. *Nanoscale* **2013**, *5*, 3149-3171.
- 751 33. Goh, K.; Karahan, H.E.; Wei, L.; Bae, T.-H.; Fane, A.G.; Wang, R.; Chen, Y. Carbon nanomaterials for
752 advancing separation membranes: A strategic perspective. *Carbon* **2016**, *109*, 694-710.
- 753 34. Gui, X.; Wei, J.; Wang, K.; Cao, A.; Zhu, H.; Jia, Y.; Shu, Q.; Wu, D. Carbon nanotube sponges. *Advanced*
754 *Materials* **2010**, *22*, 617-621.
- 755 35. Upadhyayula, V.K.K.; Deng, S.; Mitchell, M.C.; Smith, G.B. Application of carbon nanotube technology for
756 removal of contaminants in drinking water: A review. *Science of The Total Environment* **2009**, *408*, 1-13.
- 757 36. Pan, B.; Xing, B. Adsorption mechanisms of organic chemicals on carbon nanotubes. *Environmental Science*
758 *and Technology* **2008**, *42*, 9005-9013.
- 759 37. Liu, Y.; Zhang, Y.; Wang, X.; Wang, Z.; Lai, W.; Zhang, X.; Liu, X. Excellent microwave absorbing property
760 of multiwalled carbon nanotubes with skin–core heterostructure formed by outer dominated fluorination.
761 *The Journal of Physical Chemistry C* **2018**, *122*, 6357-6367.
- 762 38. Fugetsu, B.; Satoh, S.; Shiba, T.; Mizutani, T.; Lin, Y.B.; Terui, N.; Nodasaka, Y.; Sasa, K.; Shimizu, K.;
763 Akasaka, T., *et al.* Caged multiwalled carbon nanotubes as the adsorbents for affinity-based elimination of
764 ionic dyes. *Environmental Science and Technology* **2004**, *38*, 6890-6896.
- 765 39. Wu, C.H. Adsorption of reactive dye onto carbon nanotubes: Equilibrium, kinetics and thermodynamics.
766 *Journal of Hazardous Materials* **2007**, *144*, 93-100.
- 767 40. Ghaedi, M.; Shokrollahi, A.; Hossainian, H.; Kokhdan, S.N. Comparison of activated carbon and
768 multiwalled carbon nanotubes for efficient removal of eriochrome cyanine r (ecr): Kinetic, isotherm, and
769 thermodynamic study of the removal process. *Journal of Chemical and Engineering Data* **2011**, *56*, 3227-3235.
- 770 41. Shirmardi, M.; Mesdaghinia, A.; Mahvi, A.H.; Nasser, S.; Nabizadeh, R. Kinetics and equilibrium studies
771 on adsorption of acid red 18 (azo-dye) using multiwall carbon nanotubes (mwcnts) from aqueous solution.
772 *E-Journal of Chemistry* **2012**, *9*, 2371-2383.
- 773 42. Huaixu, Z.; Chunxiang, L.; Jiajun, Z.; Minghua, L.; Shiyu, F. Adsorption behavior of methylene blue on a
774 spherical cellulose adsorbent. *Trends in Carbohydrate Research* **2010**, *2*, 1-9.

- 775 43. Shahryari, Z.; Goharrizi, A.S.; Azadi, M. Experimental study of methylene blue adsorption from aqueous
776 solutions onto carbon nano tubes. *International Journal of Water Resources and Environmental Engineering*
777 **2010**, *2*, 16-28.
- 778 44. Qu, S.; Huang, F.; Yu, S.; Chen, G.; Kong, J. Magnetic removal of dyes from aqueous solution using multi-
779 walled carbon nanotubes filled with fe₂o₃particles. *Journal of Hazardous Materials* **2008**, *160*, 643-647.
- 780 45. Rodríguez, A.; Ovejero, G.; Sotelo, J.L.; Mestanza, M.; García, J. Adsorption of dyes on carbon
781 nanomaterials from aqueous solutions. *Journal of Environmental Science and Health - Part A Toxic/Hazardous*
782 *Substances and Environmental Engineering* **2010**, *45*, 1642-1653.
- 783 46. Gong, J.; Wang, B.; Zeng, G.; Yang, C.; Niu, C.; Niu, Q.; Zhou, W.; Liang, Y. Removal of cationic dyes from
784 a queous solution using magnetic multi-wall carbon nanotube nanocomposite as adsorbent. *Journal of*
785 *Hazardous Material* **2009**, *164*, 1517-1722.
- 786 47. Gao, H.; Zhao, S.; Cheng, X.; Wang, X.; Zheng, L. Removal of anionic azo dyes from aqueous solution using
787 magnetic polymer multi-wall carbon nanotube nanocomposite as adsorbent. *Chemical Engineering Journal*
788 **2013**, *223*, 84-90.
- 789 48. Ai, L.; Jiang, J. Removal of methylene blue from aqueous solution with self-assembled cylindrical graphene-
790 carbon nanotube hybrid. *Chemical Engineering Journal* **2012**, *192*, 156-163.
- 791 49. Rajabi, M.; Mahanpoor, K.; Moradi, O. Removal of dye molecules from aqueous solution by carbon
792 nanotubes and carbon nanotube functional groups: Critical review. *RSC Advances* **2017**, *7*, 47083-47090.
- 793 50. Chen, W.E.I.; Duan, L.I.N. Adsorption of polar and nonpolar organic chemicals to carbon nanotubes. **2007**,
794 *41*, 8295-8300.
- 795 51. Kun Yang, ‡; Lizhong Zhu, a.; Baoshan Xing*. Adsorption of polycyclic aromatic hydrocarbons by carbon
796 nanomaterials. *Environmental Science & Technology* **2006**, *40*, 1855-1861.
- 797 52. Agnihotri, S.; Rood, M.J.; Rostam-Abadi, M. Adsorption equilibrium of organic vapors on single-walled
798 carbon nanotubes sandeep. *carbon* **2005**, *43*, 2379-2388.
- 799 53. Crespo, D.; Yang, R.T. Adsorption of organic vapors on single-walled carbon nanotubes. *Industrial and*
800 *Engineering Chemistry Research* **2006**, *45*, 5524-5530.
- 801 54. Lu, C.; Chung, Y.L.; Chang, K.F. Adsorption of trihalomethanes from water with carbon nanotubes. *Water*
802 *Research* **2005**, *39*, 1183-1189.
- 803 55. Shao, D.; Hu, J.; Chen, C.; Sheng, G.; Ren, X.; Wang, X. Polyaniline multiwalled carbon nanotube magnetic
804 composite prepared by plasma-induced graft technique and its application for removal of aniline and
805 phenol. *Journal of Physical Chemistry C* **2010**, *114*, 21524-21530.
- 806 56. Peng, X.; Li, Y.; Luan, Z.; Di, Z.; Wang, H.; Tian, B.; Jia, Z. Adsorption of 1,2-dichlorobenzene from water
807 to carbon nanotubes. *Chemical Physics Letters* **2003**, *376*, 154-158.
- 808 57. Long, R.Q.; Yang, R.T. Carbon nanotubes as superior sorbent for dioxin removal [1]. *Journal of the American*
809 *Chemical Society* **2001**, *123*, 2058-2059.
- 810 58. Srivastava, S. Sorption of divalent metal ions from aqueous solution by oxidized carbon nanotubes and
811 nanocages: A review. *Advanced Materials Letters* **2013**, *4*, 2-8.
- 812 59. Gadhave, A.; Waghmare, J. Removal of heavy metal ions from wastewater by carbon nanotubes (cnts).
813 *International Journal of Chemical Sciences and Applications* **2014**, *5*, 56-67.
- 814 60. Rao, G.P.; Lu, C.; Su, F. Sorption of divalent metal ions from aqueous solution by carbon nanotubes: A
815 review. *Separation and Purification Technology* **2007**, *58*, 224-231.
- 816 61. Kuo, C.Y.; Lin, H.Y. Adsorption of aqueous cadmium (ii) onto modified multi-walled carbon nanotubes
817 following microwave/chemical treatment. *Desalination* **2009**, *249*, 792-796.
- 818 62. Di, Z.C.; Ding, J.; Peng, X.J.; Li, Y.H.; Luan, Z.K.; Liang, J. Chromium adsorption by aligned carbon
819 nanotubes supported ceria nanoparticles. *Chemosphere* **2006**, *62*, 861-865.
- 820 63. Chen, C.L.; Wang, X.K.; Nagatsu, M. Europium adsorption on multiwall carbon nanotube/iron oxide
821 magnetic composite in the presence of polyacrylic acid. *Environmental Science and Technology* **2009**, *43*, 2362-
822 2367.
- 823 64. Yu, F.; Wu, Y.; Ma, J.; Zhang, C. Adsorption of lead on multi-walled carbon nanotubes with different outer
824 diameters and oxygen contents: Kinetics, isotherms and thermodynamics. *Journal of Environmental Sciences*
825 *(China)* **2013**, *25*, 195-203.
- 826 65. Li, Y.H.; Di, Z.; Ding, J.; Wu, D.; Luan, Z.; Zhu, Y. Adsorption thermodynamic, kinetic and desorption
827 studies of pb₂+on carbon nanotubes. *Water Research* **2005**, *39*, 605-609.

- 828 66. Lu, C.; Liu, C. Removal of nickel(ii) from aqueous solution by carbon nanotubes. *Journal of Chemical*
829 *technology and Biotechnology* **2006**, *81*, 1932-1940.
- 830 67. Chen, C.; Wang, X. Adsorption of ni(ii) from aqueous solution using oxidized multiwall carbon nanotubes.
831 *Industrial and Engineering Chemistry Research* **2006**, *45*, 9144-9149.
- 832 68. Lu, C.; Chiu, H.; Liu, C. Removal of zinc(ii) from aqueous solution by purified carbon nanotubes: Kinetics
833 and equilibrium studies. *Industrial and Engineering Chemistry Research* **2006**, *45*, 2850-2855.
- 834 69. Lu, C.; Chiu, H. Adsorption of zinc(ii) from water with purified carbon nanotubes. *Chemical Engineering*
835 *Science* **2006**, *61*, 1138-1145.
- 836 70. Hu, B.; Fugetsu, B.; Yu, H.; Abe, Y. Prussian blue caged in spongiform adsorbents using diatomite and
837 carbon nanotubes for elimination of cesium. *Journal of Hazardous Materials* **2012**, *217-218*, 85-91.
- 838 71. Fugetsu, B.; Satoh, S.; Shiba, T.; Mizutani, T.; Lin, Y.-B.; Terui, N.; Nodasaka, Y.; Sasa, K.; Shimizu, K.;
839 Akasaka, T., *et al.* Caged multiwalled carbon nanotubes as the adsorbents for affinity-based elimination of
840 ionic dyes. *Environmental Science & Technology* **2004**, *38*, 6890-6896.
- 841 72. Fugetsu, B.; Satoh, S.; Shiba, T.; Mizutani, T.; Nodasaka, Y.; Yamazaki, K.; Shimizu, K.; Shindoh, M.; Shibata,
842 K.-i.; Nishi, N., *et al.* Large-scale production of ba²⁺-alginate-coated vesicles of carbon nanofibers for DNA-
843 interactive pollutant elimination. *Bulletin of the Chemical Society of Japan* **2004**, *77*, 1945-1950.
- 844 73. Yu, H.; Fugetsu, B. A novel adsorbent obtained by inserting carbon nanotubes into cavities of diatomite
845 and applications for organic dye elimination from contaminated water. *Journal of Hazardous Materials* **2010**,
846 *177*, 138-145.
- 847 74. Lin, Y.-B.; Fugetsu, B.; Terui, N.; Tanaka, S. Removal of organic compounds by alginate gel beads with
848 entrapped activated carbon. *Journal of Hazardous Materials* **2005**, *120*, 237-241.
- 849 75. Wang, Y.; Wang, J.; Morimoto, S.; Hong Melvin, G.J.; Zhao, R.; Hashimoto, Y.; Terrones, M. Nitrogen-doped
850 porous carbon monoliths from molecular-level dispersion of carbon nanotubes into polyacrylonitrile (pan)
851 and the effect of carbonization process for supercapacitors. *Carbon* **2019**, *143*, 776-785.
- 852 76. Wang, Y.; Fugetsu, B.; Wang, Z.; Gong, W.; Sakata, I.; Morimoto, S.; Hashimoto, Y.; Endo, M.; Dresselhaus,
853 M.; Terrones, M. Nitrogen-doped porous carbon monoliths from polyacrylonitrile (pan) and carbon
854 nanotubes as electrodes for supercapacitors. *Scientific Report* **2017**, *7*, 40259.
- 855 77. Wang, Y.; Fugetsu, B. Mono-dispersed ultra-long single-walled carbon nanotubes as enabling components
856 in transparent and electrically conductive thin films. *Carbon* **2015**, *82*, 152-160.
- 857 78. Fugetsu, B.; Satoh, S.; Shiba, T.; Mizutani, T.; Lin, Y.B.; Terui, N.; Nodasaka, Y.; Sasa, K.; Shimizu, K.;
858 Akasaka, R., *et al.* Caged multiwalled carbon nanotubes as the adsorbents for affinity-based elimination of
859 ionic dyes. *Environmental Science & Technology* **2004**, *38*, 6890-6896.
- 860 79. Vipin, A.K.; Ling, S.; Fugetsu, B. Removal of cs⁺ and sr²⁺ from water using mwcnt reinforced zeolite-a
861 beads. *MICROPOROUS AND MESOPOROUS MATERIALS* **2016**, *224*, 84-88.
- 862 80. Vipin, A.K.; Ling, S.; Fugetsu, B. Sodium cobalt hexacyanoferrate encapsulated in alginate vesicle with cnt
863 for both cesium and strontium removal. *Carbohydrate Polymers* **2014**, *111*, 477-484.
- 864 81. He, J.; Yu, H.; Fugetsu, B.; Tanaka, S.; Sun, L. Electrochemical removal of bisphenol a using a cnt-covered
865 polyester yarn electrode. *SEPARATION AND PURIFICATION TECHNOLOGY* **2013**, *110*, 81-85.
- 866 82. Vipin, A.K.; Hu, B.; Fugetsu, B. Prussian blue caged in alginate/calcium beads as adsorbents for removal of
867 cesium ions from contaminated water. *Journal of Hazardous Materials* **2013**, *258-259*, 93-101.
- 868 83. Carey, J.H.; Lawrence, J.; Tosine, H.M. Photodechlorination of pcb's in the presence of titanium dioxide in
869 aqueous suspensions. *Bulletin of Environmental Contamination and Toxicology* **1976**, *16*, 697-701.
- 870 84. Mills, A.; Le Hunte, S. An overview of semiconductor photocatalysis. *Journal of Photochemistry and*
871 *Photobiology A: Chemistry* **1997**, *108*, 1-35.
- 872 85. Zou, Z.; Ye, J.; Sayama, K.; Arakawa, H. Direct splitting of water under visible light irradiation with an
873 oxide semiconductor photocatalyst. *Nature* **2001**, *414*, 625.
- 874 86. Fagan, R.; McCormack, D.E.; Dionysiou, D.D.; Pillai, S.C. A review of solar and visible light active tio₂
875 photocatalysis for treating bacteria, cyanotoxins and contaminants of emerging concern. *Materials Science*
876 *in Semiconductor Processing* **2016**, *42*, 2-14.
- 877 87. Pu, S.; Hou, Y.; Chen, H.; Deng, D.; Yang, Z.; Xue, S.; Zhu, R.; Diao, Z.; Chu, W. An efficient photocatalyst
878 for fast reduction of cr(vi) by ultra-trace silver enhanced titania in aqueous solution. *Catalysts* **2018**, *8*, 251.
- 879 88. Asahi, R.; Morikawa, T.; Ohwaki, T.; Aoki, K.; Taga, Y. Visible-light photocatalysis in nitrogen-doped
880 titanium oxides. *Science* **2001**, *293*, 269-271.

- 881 89. Xu, Y.-J.; Zhuang, Y.; Fu, X. New insight for enhanced photocatalytic activity of tio₂ by doping carbon
882 nanotubes: A case study on degradation of benzene and methyl orange. *The Journal of Physical Chemistry C*
883 **2010**, *114*, 2669-2676.
- 884 90. Woan, K.; Pyrgiotakis, G.; Sigmund, W. Photocatalytic carbon-nanotube–tio₂ composites. *Advanced*
885 *Materials* **2009**, *21*, 2233-2239.
- 886 91. Ge, M.; Li, Q.; Cao, C.; Huang, J.; Li, S.; Zhang, S.; Chen, Z.; Zhang, K.; Al-Deyab, S.S.; Lai, Y. One-
887 dimensional tio₂ nanotube photocatalysts for solar water splitting. *Advanced Science* **2017**, *4*, 1600152.
- 888 92. Wang, Q.; Wang, Y.; Duan, B.; Zhang, M. Modified sol-gel synthesis of carbon nanotubes supported titania
889 composites with enhanced visible light induced photocatalytic activity. *Journal of Nanomaterials* **2016**, *2016*,
890 6.
- 891 93. Li, J.; Zhou, Y.; Xiao, X.; Wang, W.; Wang, N.; Qian, W.; Chu, W. Regulation of ni–cnt interaction on mn-
892 promoted nickel nanocatalysts supported on oxygenated cnts for co₂ selective hydrogenation. *ACS Applied*
893 *Materials & Interfaces* **2018**, *10*, 41224-41236.
- 894 94. Gao, S.J.; Shi, Z.; Zhang, W.B.; Zhang, F.; Jin, J. Photoinduced superwetting single-walled carbon
895 nanotube/tio₂ ultrathin network films for ultrafast separation of oil-in-water emulsions. *ACS Nano* **2014**, *8*,
896 6344-6352.
- 897 95. Park, H.-A.; Liu, S.; Salvador, P.A.; Rohrer, G.S.; Islam, M.F. High visible-light photochemical activity of
898 titania decorated on single-wall carbon nanotube aerogels. *RSC Advances* **2016**, *6*, 22285-22294.
- 899 96. Zhao, D.; Yang, X.; Chen, C.; Wang, X. Enhanced photocatalytic degradation of methylene blue on
900 multiwalled carbon nanotubes–tio₂. *Journal of Colloid and Interface Science* **2013**, *398*, 234-239.
- 901 97. Lee, W.J.; Lee, J.M.; Kochuveedu, S.T.; Han, T.H.; Jeong, H.Y.; Park, M.; Yun, J.M.; Kwon, J.; No, K.; Kim,
902 D.H., *et al.* Biomineralized n-doped cnt/tio₂ core/shell nanowires for visible light photocatalysis. *ACS Nano*
903 **2012**, *6*, 935-943.
- 904 98. Liu, Y.; Li, F.; Xia, Q.; Wu, J.; Liu, J.; Huang, M.; Xie, J. Conductive 3d sponges for affordable and highly-
905 efficient water purification. *Nanoscale* **2018**, *10*, 4771-4778.
- 906 99. Xu, Z.; Liu, H.; Niu, J.; Zhou, Y.; Wang, C.; Wang, Y. Hydroxyl multi-walled carbon nanotube-modified
907 nanocrystalline pbo₂ anode for removal of pyridine from wastewater. *Journal of Hazardous Materials* **2017**,
908 327, 144-152.
- 909 100. Moronshing, M.; Subramaniam, C. Scalable approach to highly efficient and rapid capacitive deionization
910 with cnt-thread as electrodes. *ACS Applied Materials & Interfaces* **2017**, *9*, 39907-39915.
- 911 101. Huang, J.; Liu, H.; Chen, S.; Ding, C. Hierarchical porous mwcnts-silica aerogel synthesis for high-efficiency
912 oily water treatment. *Journal of Environmental Chemical Engineering* **2016**, *4*, 3274-3282.
- 913 102. Duan, X.; Sun, H.; Wang, Y.; Kang, J.; Wang, S. N-doping-induced nonradical reaction on single-walled
914 carbon nanotubes for catalytic phenol oxidation. *ACS Catalysis* **2015**, *5*, 553-559.
- 915 103. Banerjee, S.; Wong, S.S. Synthesis and characterization of carbon nanotube–nanocrystal heterostructures.
916 *Nano Letters* **2002**, *2*, 195-200.
- 917 104. Yang, Y.; Qu, L.; Dai, L.; Kang, T.-S.; Durstock, M. Electrophoresis coating of titanium dioxide on aligned
918 carbon nanotubes for controlled syntheses of photoelectronic nanomaterials. *Advanced Materials* **2007**, *19*,
919 1239-1243.
- 920 105. Daghri, R.; Drogui, P.; Robert, D. Modified tio₂ for environmental photocatalytic applications: A review.
921 *Industrial & Engineering Chemistry Research* **2013**, *52*, 3581-3599.
- 922 106. Konstantinou, I.K.; Albanis, T.A. Tio₂-assisted photocatalytic degradation of azo dyes in aqueous solution:
923 Kinetic and mechanistic investigations: A review. *Applied Catalysis B: Environmental* **2004**, *49*, 1-14.
- 924 107. Yao, Y.; Li, G.; Ciston, S.; Lueptow, R.M.; Gray, K.A. Photoreactive tio₂/carbon nanotube composites:
925 Synthesis and reactivity. *Environmental Science & Technology* **2008**, *42*, 4952-4957.
- 926 108. Chen, G. Electrochemical technologies in wastewater treatment. *Separation and Purification Technology* **2004**,
927 38, 11-41.
- 928 109. Moreira, F.C.; Boaventura, R.A.R.; Brillas, E.; Vilar, V.J.P. Electrochemical advanced oxidation processes: A
929 review on their application to synthetic and real wastewaters. *Applied Catalysis B: Environmental* **2017**, *202*,
930 217-261.
- 931 110. Al-Rowaili, F.N.; Jamal, A.; Ba Shammakh, M.S.; Rana, A. A review on recent advances for electrochemical
932 reduction of carbon dioxide to methanol using metal–organic framework (mof) and non-mof catalysts:
933 Challenges and future prospects. *ACS Sustainable Chemistry & Engineering* **2018**, *6*, 15895-15914.

- 934 111. Martínez-Huitile, C.A.; Rodrigo, M.A.; Sirés, I.; Scialdone, O. Single and coupled electrochemical processes
935 and reactors for the abatement of organic water pollutants: A critical review. *Chemical Reviews* **2015**, *115*,
936 13362-13407.
- 937 112. Radjenovic, J.; Sedlak, D.L. Challenges and opportunities for electrochemical processes as next-generation
938 technologies for the treatment of contaminated water. *Environmental Science & Technology* **2015**, *49*, 11292-
939 11302.
- 940 113. Rahaman, M.S.; Vecitis, C.D.; Elimelech, M. Electrochemical carbon-nanotube filter performance toward
941 virus removal and inactivation in the presence of natural organic matter. *Environmental Science & Technology*
942 **2012**, *46*, 1556-1564.
- 943 114. Panizza, M.; Cerisola, G. Direct and mediated anodic oxidation of organic pollutants. *Chemical Reviews* **2009**,
944 *109*, 6541-6569.
- 945 115. Rüetschi, P.; Cahan, B.D. Electrochemical properties of pbo2 and the anodic corrosion of lead and lead
946 alloys. *Journal of The Electrochemical Society* **1958**, *105*, 369-377.
- 947 116. Guan, C.; Jiang, J.; Pang, S.; Luo, C.; Ma, J.; Zhou, Y.; Yang, Y. Oxidation kinetics of bromophenols by
948 nonradical activation of peroxydisulfate in the presence of carbon nanotube and formation of brominated
949 polymeric products. *Environmental Science & Technology* **2017**, *51*, 10718-10728.
- 950 117. Lee, H.; Lee, H.-J.; Jeong, J.; Lee, J.; Park, N.-B.; Lee, C. Activation of persulfates by carbon nanotubes:
951 Oxidation of organic compounds by nonradical mechanism. *Chemical Engineering Journal* **2015**, *266*, 28-33.
- 952 118. Kyzas, G.Z.; Deliyanni, E.A.; Matis, K.A. Graphene oxide and its application as an adsorbent for wastewater
953 treatment. *Journal of Chemical Technology & Biotechnology* **2014**, *89*, 196-205.
- 954 119. Huang, J.; Zheng, Y.; Luo, L.; Feng, Y.; Zhang, C.; Wang, X.; Liu, X. Facile preparation of highly hydrophilic,
955 recyclable high-performance polyimide adsorbents for the removal of heavy metal ions. *Journal of*
956 *Hazardous Materials* **2016**, *306*, 210-219.
- 957 120. Sun, L.; Yu, H.; Fugetsu, B. Graphene oxide adsorption enhanced by in situ reduction with sodium
958 hydrosulfite to remove acridine orange from aqueous solution. *Journal of Hazardous Materials* **2012**, *203-204*,
959 101-110.
- 960 121. Sun, L.; Fugetsu, B. Graphene oxide captured for green use: Influence on the structures of calcium alginate
961 and macroporous alginic beads and their application to aqueous removal of acridine orange. *Chemical*
962 *Engineering Journal* **2014**, *240*, 565-573.
- 963 122. Lai, W.; Liu, J.; Luo, L.; Wang, X.; He, T.; Fan, K.; Liu, X. The friedel-crafts reaction of fluorinated graphene
964 for high-yield arylation of graphene. *Chemical Communications* **2018**, *54*, 10168-10171.
- 965 123. Wang, S.; Li, X.; Liu, Y.; Zhang, C.; Tan, X.; Zeng, G.; Song, B.; Jiang, L. Nitrogen-containing amino
966 compounds functionalized graphene oxide: Synthesis, characterization and application for the removal of
967 pollutants from wastewater: A review. *Journal of hazardous materials* **2018**, *342*, 177-191.
- 968 124. Sun, L.; Fugetsu, B. Mass production of graphene oxide from expanded graphite. *Materials Letters* **2013**, *109*,
969 207-210.
- 970 125. Konicki, W.; Aleksandrak, M.; Moszynski, D.; Mijowska, E. Adsorption of anionic azo-dyes from aqueous
971 solutions onto graphene oxide: Equilibrium, kinetic and thermodynamic studies. *JOURNAL OF COLLOID*
972 *AND INTERFACE SCIENCE* **2017**, *496*, 188-200.
- 973 126. Robati, D.; Mirza, B.; Rajabi, M.; Moradi, O.; Tyagi, I.; Agarwal, S.; Gupta, V.K. Removal of hazardous dyes-
974 br 12 and methyl orange using graphene oxide as an adsorbent from aqueous phase. *Chemical Engineering*
975 *Journal* **2016**, *284*, 687-697.
- 976 127. Du, Q.; Sun, J.; Li, Y.; Yang, X.; Wang, X.; Wang, Z.; Xia, L. Highly enhanced adsorption of congo red onto
977 graphene oxide/chitosan fibers by wet-chemical etching off silica nanoparticles. *Chemical Engineering*
978 *Journal* **2014**, *245*, 99-106.
- 979 128. Wu, Z.; Zhong, H.; Yuan, X.; Wang, H.; Wang, L.; Chen, X.; Zeng, G.; Wu, Y. Adsorptive removal of
980 methylene blue by rhamnolipid-functionalized graphene oxide from wastewater. *Water Research* **2014**, *67*,
981 330-344.
- 982 129. Cheng, C.; Deng, J.; Lei, B.; He, A.; Zhang, X.; Ma, L.; Li, S.; Zhao, C. Toward 3d graphene oxide gels based
983 adsorbents for high-efficient water treatment via the promotion of biopolymers. *Journal of hazardous*
984 *materials* **2013**, *263*, 467-478.
- 985 130. Li, Y.; Du, Q.; Liu, T.; Peng, X.; Wang, J.; Sun, J.; Wang, Y.; Wu, S.; Wang, Z.; Xia, Y., et al. Comparative
986 study of methylene blue dye adsorption onto activated carbon, graphene oxide, and carbon nanotubes.
987 *Chemical Engineering Research & Design* **2013**, *91*, 361-368.

- 988 131. Tiwari, J.N.; Mahesh, K.; Le, N.H.; Kemp, K.C.; Timilsina, R.; Tiwari, R.N.; Kim, K.S. Reduced graphene
989 oxide-based hydrogels for the efficient capture of dye pollutants from aqueous solutions. *CARBON* **2013**,
990 *56*, 173–182.
- 991 132. Liu, F.; Chung, S.; Oh, G.; Seo, T.S. Three-dimensional graphene oxide nanostructure for fast and efficient
992 water-soluble dye removal. *Acs Applied Materials & Interfaces* **2012**, *4*, 922–927.
- 993 133. Huang, Y.; Ruan, G.; Ruan, Y.; Zhang, W.; Li, X.; Du, F.; Hu, C.; Li, J. Hypercrosslinked porous polymers
994 hybridized with graphene oxide for water treatment: Dye adsorption and degradation. *Rsc Advances* **2018**,
995 *8*, 13417–13422.
- 996 134. Lv, M.; Yan, L.; Liu, C.; Su, C.; Zhou, Q.; Zhang, X.; Lan, Y.; Zheng, Y.; Lai, L.; Liu, X., *et al.* Non-covalent
997 functionalized graphene oxide (go) adsorbent with an organic gelator for co-adsorption of dye, endocrine-
998 disruptor, pharmaceutical and metal ion. *Chemical Engineering Journal* **2018**, *349*, 791–799.
- 999 135. Wang, H.; Wei, Y. Magnetic graphene oxide modified by chloride imidazole ionic liquid for the high-
1000 efficiency adsorption of anionic dyes. *Rsc Advances* **2017**, *7*, 9079–9089.
- 1001 136. Wu, X.-L.; Xiao, P.; Zhong, S.; Fang, K.; Lin, H.; Chen, J. Magnetic znfe₂o₄@chitosan encapsulated in
1002 graphene oxide for adsorptive removal of organic dye. *Rsc Advances* **2017**, *7*, 28145–28151.
- 1003 137. Faghihi, A.; Vakili, M.H.; Hosseinzadeh, G.; Farhadian, M.; Jafari, Z. Synthesis and application of recyclable
1004 magnetic freeze-dried graphene oxide nanocomposite as a high capacity adsorbent for cationic dye
1005 adsorption. *Desalination and Water Treatment* **2016**, *57*, 22655–22670.
- 1006 138. Sahraei, R.; Hemmati, K.; Ghaemy, M. Adsorptive removal of toxic metals and cationic dyes by magnetic
1007 adsorbent based on functionalized graphene oxide from water. *Rsc Advances* **2016**, *6*, 72487–72499.
- 1008 139. Gan, L.; Shang, S.; Hu, E.; Wah, C.; Yuen, M.; Jiang, S.-x. Konjac glucomannan/graphene oxide hydrogel
1009 with enhanced dyes adsorption capability for methyl blue and methyl orange. *Applied Surface Science* **2015**,
1010 *357*, 866–872.
- 1011 140. Coello-Fiallos, D.; Cazzanelli, E.; Tavolaro, A.; Tavolaro, P.; Arias, M.; Caputi, L.S. Cresyl violet adsorption
1012 on sonicated graphite oxide. *Journal of Nanoscience and Nanotechnology* **2018**, *18*, 3006–3011.
- 1013 141. You, Y.; Sahajwalla, V.; Yoshimura, M.; Joshi, R.K. Graphene and graphene oxide for desalination. *Nanoscale*
1014 **2016**, *8*, 117–119.
- 1015 142. Jiao, X.; Zhang, L.; Qiu, Y.; Guan, J. Comparison of the adsorption of cationic blue onto graphene oxides
1016 prepared from natural graphites with different graphitization degrees. *Colloids and Surfaces A-
1017 Physicochemical and Engineering Aspects* **2017**, *529*, 292–301.
- 1018 143. Ghaedi, M.; Zeinali, N.; Ghaedi, A.M.; Teimuori, M.; Tashkhourian, J. Artificial neural network-genetic
1019 algorithm based optimization for the adsorption of methylene blue and brilliant green from aqueous
1020 solution by graphite oxide nanoparticle. *Spectrochimica Acta Part A-Molecular and Biomolecular Spectroscopy*
1021 **2014**, *125*, 264–277.
- 1022 144. He, G.; Zhang, J.; Zhang, Y.; Chen, H.; Wang, X. Fast and efficient removal of cationic dye using graphite
1023 oxide, adsorption, and kinetics studies. *Journal of Dispersion Science and Technology* **2013**, *34*, 1223–1229.
- 1024 145. Jin, Q.-Q.; Zhu, X.-H.; Xing, X.-Y.; Ren, T.-Z. Adsorptive removal of cationic dyes from aqueous solutions
1025 using graphite oxide. *Adsorption Science & Technology* **2012**, *30*, 437–447.
- 1026 146. Bradder, P.; Ling, S.K.; Wang, S.; Liu, S. Dye adsorption on layered graphite oxide. *Journal of Chemical and
1027 Engineering Data* **2011**, *56*, 138–141.
- 1028 147. Wang, J.; Chen, B.; Xing, B. Wrinkles and folds of activated graphene nanosheets as fast and efficient
1029 adsorptive sites for hydrophobic organic contaminants. *Environmental science & technology* **2016**, *50*, 3798–
1030 3808.
- 1031 148. Fiallos, D.C.; Gómez, C.V.; Usca, G.T.; Pérez, D.C.; Tavolaro, P.; Martino, G.; Caputi, L.S.; Tavolaro, A.
1032 Removal of acridine orange from water by graphene oxide. 2015; pp 38–45.
- 1033 149. Liu, J.; Li, P.; Xiao, H.; Zhang, Y.; Shi, X.; Lü, X.; Chen, X. Understanding flocculation mechanism of
1034 graphene oxide for organic dyes from water: Experimental and molecular dynamics simulation. *AIP
1035 Advances* **2015**, *5*, 117151.
- 1036 150. Zhang, X.; Yu, H.; Yang, H.; Wan, Y.; Hu, H.; Zhai, Z.; Qin, J. Graphene oxide caged in cellulose microbeads
1037 for removal of malachite green dye from aqueous solution. *JOURNAL OF COLLOID AND INTERFACE
1038 SCIENCE* **2015**, *437*, 277–282.
- 1039 151. Fugetsu, B.; Sano, E.; Yu, H.; Mori, K.; Tanaka, T. Graphene oxide as dyestuffs for the creation of electrically
1040 conductive fabrics. *Carbon* **2010**, *48*, 3340–3345.

- 1041 152. Wang, Y.; Sun, L.; Fugetsu, B. Thiourea dioxide as a green reductant for the mass production of solution-
1042 based graphene. *Bulletin of the Chemical Society of Japan* **2012**, *85*, 1339-1344.
- 1043 153. Yokwana, K.; Kuvarega, A.T.; Mhlanga, S.D.; Nxumalo, E.N. Mechanistic aspects for the removal of congo
1044 red dye from aqueous media through adsorption over n-doped graphene oxide nanoadsorbents prepared
1045 from graphite flakes and powders. *Physics and Chemistry of the Earth* **2018**, *107*, 58–70.
- 1046 154. Fiallos, D.C.; Gómez, C.V.; Usca, G.T.; Pérez, D.C.; Tavolaro, P.; Martino, G.; Caputi, L.S.; Tavolaro, A. In
1047 *Removal of acridine orange from water by graphene oxide*, International Conferences and Exhibition on
1048 Nanotechnologies and Organic Electronics (NANOTECHNOLOGY 2014), 2015; the American Institute of
1049 Physics: pp 38–45.
- 1050 155. Sabzevari, M.; Cree, D.E.; Wilson, L.D. Graphene oxide–chitosan composite material for treatment of a
1051 model dye effluent. *Acs Omega* **2018**, *3*, 13045–13054.
- 1052 156. Wang, H.; Chen, Y.; Wei, Y. A novel magnetic calcium silicate/graphene oxide composite material for
1053 selective adsorption of acridine orange from aqueous solutions. *Rsc Advances* **2016**, *6*, 34770–34781.
- 1054 157. Kovtyukhova, N.I.; Ollivier, P.J.; Martin, B.R.; Mallouk, T.E.; Chizhik, S.A.; Buzaneva, E.V.; Gorchinskiy,
1055 A.D. Layer-by-layer assembly of ultrathin composite films from micron-sized graphite oxide sheets and
1056 polycations. *Chem. Mater.* **1999**, *11*, 771–778.
- 1057 158. Hummers, W.S.; Offeman, R.E. Preparation of graphitic oxide. *J. Am. Chem. Soc.* **1958**, *80*, 1339.
- 1058 159. Liu, B.; Guo, W.; Ren, N. Decontamination of wastewaters containing synthetic organic dyes by
1059 electrochemical methods: A review. *Advanced Research on Material Engineering, Chemistry and Environment*
1060 **2013**, *788*, 405–408.
- 1061 160. Yang, H.; Li, H.; Zhai, J.; Sun, L.; Yu, H. Simple synthesis of graphene oxide using ultrasonic cleaner from
1062 expanded graphite. *INDUSTRIAL & ENGINEERING CHEMISTRY RESEARCH* **2014**, *53*, 17878–17883.
- 1063 161. Ahmad, H.; Fan, M.; Hui, D. Graphene oxide incorporated functional materials: A review. *Composites Part*
1064 *B: Engineering* **2018**, *145*, 270-280.
- 1065 162. Li, F.; Jiang, X.; Zhao, J.; Zhang, S. Graphene oxide: A promising nanomaterial for energy and
1066 environmental applications. *Nano Energy* **2015**, *16*, 488-515.
- 1067 163. Chabot, V.; Higgins, D.; Yu, A.; Xiao, X.; Chen, Z.; Zhang, J. A review of graphene and graphene oxide
1068 sponge: Material synthesis and applications to energy and the environment. *Energy & Environmental Science*
1069 **2014**, *7*, 1564-1596.
- 1070 164. Wang, Y.; Sun, L.; Fugetsu, B. Morphology-controlled synthesis of sunlight-driven plasmonic
1071 photocatalysts ag@agx (x = cl, br) with graphene oxide template. *Journal of Materials Chemistry A* **2013**, *1*,
1072 12536-12544.
- 1073 165. Wang, Y.; Fugetsu, B.; Sakata, I.; Mao, W.; Endo, M.; Terrones, M.; Dresselhaus, M. Preparation of novel
1074 tetrahedral ag₃po₄ crystals and the sunlight-responsive photocatalytic properties using graphene oxide as
1075 the template. *Carbon* **2017**, *119*, 522-526.
- 1076 166. Wang, Y.; Fugetsu, B.; Sakata, I.; Terrones, M.; Endo, M.; Dresselhaus, M. Morphology-controlled
1077 fabrication of a three-dimensional mesoporous poly(vinyl alcohol) monolith through the incorporation of
1078 graphene oxide. *Carbon* **2016**, *98*, 334-342.
- 1079 167. Huang, Y.; Zeng, M.; Chen, J.; Wang, Y.; Xu, Q. Multi-structural network design and mechanical properties
1080 of graphene oxide filled chitosan-based hydrogel nanocomposites. *Materials & Design* **2018**, *148*, 104-114.
- 1081 168. Wang, Y.; Fugetsu, B. A polyelectrolyte-stabilized approach for massive production of agcl/graphene
1082 nanocomposites. *Chemistry Letters* **2013**, *42*, 438-440.
- 1083



© 2019 by the authors. Submitted for possible open access publication under the terms and conditions of the Creative Commons Attribution (CC BY) license (<http://creativecommons.org/licenses/by/4.0/>).